Reactive Equity Pricing: Connecting Equity Price Changes to Changes in the Macrofinance 'State of Risk'

RONALD A BLANKEN*

Abstract

The 3MR Reactive Price Model (Model) employs a two-step procedure to predict future values of the S&P 500 index. First, an investor in the current timestep predicts how a future investor will value the equity using a linear regression, which calculates the reactive response of the current yield to expected changes in 3 stationary (almost) uncorrelated Macro Risks: the one-year treasury bond rate, the consumer confidence index, and the trailing cash reference growth rate (together, the macrofinance 'state of risk.') Second, the investor applies the yield prediction to the expected cash reference variable (either the earnings or dividend) to make the price prediction. Price prediction is possible because the reactive model rejects the martingale hypothesis, which allows a backward-looking yield estimate. Sequential application of the Model predicts the response of the price to changes in the 'state of risk' over the next twelve months. Using E/P, Model responses broadly follow the large price changes that occurred during CY1987 and the eight regressions in the database (1967:2023). A Model extension assumes that the future investor who sets the price loses memory of the current yield as the prediction horizon increases; this helps explain the persistence of the high prices that occurred during the late 1990s. The significant size of the Model's prediction error limits but does not preclude investor application.

*Sci2Tech, Inc., email: blanken@sci2tech.com

1. Introduction

In 1965, Samuelson published a seminal paper entitled "Proof That Properly Anticipated Prices Fluctuate Randomly." By "Properly Anticipated," Samuelson meant prices follow a martingale[1] process. Black and Sholes (1972) assumed the price follows a martingale process specified by the stochastic differential equation $\Delta P=\mu P+N(0, \sigma)$ where μ is the growth rate and $N()$ is a Brownian Motion process. They derived an analytic expression for the risk-neutral option price and the amount of the underlying that a dealer would need to maintain a risk-free hedge. Black Scholes found an analytic solution to the ΔP stochastic differential equation, a probability density whose mean grows as $e^{\mu t}$ with a volatility moment that increases as σ*sqrt(t). The economic source of the volatility (σ) is unknown.

Under the martingale hypothesis, equity prices vary randomly. The only way to disprove the martingale hypothesis is through an equity price model (the familiar Efficient Market Joint Hypothesis challenge). This paper develops an equity price model that links equity price changes with changes in key macroeconomic data variables, disproving the martingale hypothesis.

To predict equity price, the investor must put himself 'in the shoes' of an investor at a forward point in time who sets the price using the data set available to her at the forward time. If the investor is forward-looking and sets the price by discounting expected dividends, a prediction for the future investor's valuation would require an assumption for expectations of expectations, which rational expectations do not allow.

---

[1] Wikipedia: A statistical martingale process is a sequence of random variables where the expected value of the next variable, given all past variables, is equal to the current value.

In this paper, I develop a Reactive Yield Model that does not assume the martingale hypothesis, making valuation predictions without the need for expectations of expectations possible. The Reactive Yield Model assumes there is a yield function $Y(\$X/P_{t-1},\$X/P_{t-2}, ..,xiN_t,xiN_{t-1},\ldots)$ having both reported *normalized* data variables ($xiN_{t,\ldots}$) and trailing yields ($\$X/P_{t-1},\ldots$) in its dataset, which returns a yield prediction $(\$X/P)_{Prdict.t}$. The inclusion of the trailing data and yields nullifies the martingale hypothesis. To estimate the price, the investor applies the yield estimate to $Xt [$Pt=\$Xt/(\$X/P)_{Predict.t}$].

If Y( ) were a mathematical function, a Taylor expansion about $\$X/P_t$ calculates the first-order changes ΔY_{t+n} due to first-order changes in the xiN (ΔxiN_{t+n}). A priori, the structure of Y( ) is unknown. Instead, because the dataset contains the first-order responses, the Reactive Yield Model uses the linear regression

$$Y_{\Delta xiN.t->t+n} = lm(\$X/P_t \sim \text{'0'} + \$X/P_t + \Sigma\, ß_{\Delta xiN.t->t+n} * \Delta xiN_{t->t+n})$$

to calculate the strengths (the $ß_{\Delta xiN.t+n}$) of first-order responses of $\Delta\$X/P$ to the Taylor shocks $\Delta xiN_{t->t+n} = xiN_{t+n} - xiN_t$ (the '0' instructs the software to exclude a regression constant). The $Y_{\Delta xiN.t->t+n}$ regression is a time series implementation of a Taylor expansion of a mathematical function. There is an arrow of time imposed by the requirement that the **T**arget timestep (t+n) is in the future relative to the shock's **O**rigen timestep (t). An investor can set the current timestep t_0 to either the Target or Origin timestep. The Taylor shock assumes the data variables are perfectly autocorrelated, as in a mathematical Taylor expansion. The Taylor regression illustrates the primary features of the reactive approach to equity pricing.

'Priced' variables can only be determined within the context of a Price Model. This paper uses the risk-adjusted prices defined by $P \equiv (P_{begin} + P_{high} + P_{low} + P_{end})/4$ (see Appendix A.1); this definition reduces the price volatility compared to the volatility in the Black-Scholes model, which

incorporates infratemporal volatility. Useful data variables must be stationary and have high covariance with X/P_{Data}. Additionally, if the 'priced' variables are quasi-orthogonal, the yield response becomes decomposable into the contribution from each shock. An empirical search using an extended historical database (1967:1-2023:12) identified three macroeconomic data variables with the requisite properties: the one-year treasury bond rate (tcm1yN), the 12-month trailing cash flow growth rate ($XGN), and the Consumer Confidence Index (cciN). [Appendix A.1 explains the construction of the S&P 500 earnings data series.]. Collectively, the Model refers to these data variables as the 3 Macro Risks (3MR) because a change in any of them could potentially alter $X/P in a way that decreases the price of the market portfolio. The triplet 3MRi[3] = ($tcm1yN_t$,$\$XGN_t$,$cciN_t$) defines the 'state of risk' of the macrofinance economy. Because the 3MRi risk variables are among the most widely discussed variables responsible for price changes in the financial press, there should be no question of their relevance (Chinco et al., 2022).

When the Targeted investor is in the current timestep t_0, the reactive pricing process closely mirrors the pricing process described in the financial press, where investors await the reports of critical macroeconomic data variables. The 3MRi reports are asynchronous, partially explaining the sizeable infratemporal price volatility. In the Reactive Yield Model, "Properly Anticipated" (the martingale property) applies exclusively to the time step where the investor receives the shock. If investors anticipate the $3MRi_t$ report and adjust the price before the $3MRi_t$ report, the price remains unchanged (does not vary randomly) upon the $3MRi_t$ report. Conversely, if investors do not anticipate $3MR_t$, the price changes upon the $3MRi_t$ report. Either way, investors incorporate the shock into the yield in the time step when the data report is received. The infratemporal martingale property precludes the use of event studies to identify 'priced' data variables, explaining market efficiency.

In the predictive case where t_0 is the Origin time step, investors put themselves 'in the shoes' of an investor at the future point in time (at horizon n) who uses the current investors' expectations for the $3MRi_{t+n}$ to calculate $\Delta Y_{\Delta 3MRi.t->t+n}$ as the response to the Taylor shock $\Delta xiN_{Taylor.i.n} = (3MRi_{t+n} - 3MRi_t)$ whose Origin is in current time step. In the predictive case, because the Origin investor is always in the current time step, the Model omits the time (t) identifier as it is unnecessary. The forward investor applies the predicted yield $Y_{\Delta 3MR.n}$ to the current investor's expectation for $\$X._n$ to calculate $P._n$.

The forward time history of $X/PData.n is determined by investors' reactions to changes in the 3MRi originating in the previous timestep $\Delta 3MRi_{t+n-1->t+n}$. An investor could predict the price history by sequentially applying $Y_{\Delta 3MRit+n-1->t+n}$ to investors' expectations for the $3MRi._n$. Because there is an error in each time step's prediction, the prediction error increases as sqrt(n).

The Taylor regression assumes that the Origin and the target variables are perfectly auto-correlated. In practice, investors are less likely to value the Origin Data variable less than the Target variable. Requiring separate regression coefficients for the Origin ($ß._O$) and Target ($ß._T$) shock variables implements a loss of memory of the Origen risk variable into the Full Reactive Yield Model ($Y_{\Delta 3MR.Full.\$X.n}$).

$$\Delta xiN_{Full.n} \equiv \beta_{T.i.n} xiN_{t+n} - \beta_{O.i.n} xiN_t$$

The Full Reactive Yield Regression includes a regression constant. There are two limits: At short horizons, 'Const' = 0 and $ß_{\Delta 3MRi.t} = (-1)* ß_{\Delta 3MRi.t+n}$, and the regression becomes a time series implementation of a *Taylor* expansion of a mathematical function ($Y_{\Delta 3MRi.Taylor.n}$) At large horizons when investors lose their memory of the Origin data variable ($\beta_{O.i.n}$), the 'Const'= <$X/P>, and the regression Y_{3MR} becomes *Static* (i.e., it has no horizon dependence.) Unless required, we assume the use of the Full Model and omit the regression label (e.g., $Y_{\Delta 3MR.\$X.n}$).

The StdDev($\Delta\$X/P_{Data.n}$) increases as the horizon increases. In the Reactive Yield Model, the responses to risk ($ß_{\Delta 3MRi.n}$) similarly increase. Unlike the Black Scholes Model, where the volatility (σ*sqrt(t)) continues to grow with the horizon, in the $Y_{\Delta 3MR.n}$ Model, as the volatility prediction StdDev($\Delta\$X/P_{.Predict.n}$) approaches StdDev($X/P), the $Y_{\Delta 3MR.n}$ prediction saturates because the predicted volatility cannot exceed the volatility of the X/P_t$ database.

The 3MR Reactive Price Model predicts the price (P)

$$P_{\Delta 3MR.\$X.n} \equiv \frac{\$X.n}{Y_{\Delta 3MR.\$X.n}}$$

The Model assumes the investor knows X.n with certainty, so the price prediction error is entirely the result of the $Y_{\Delta 3MR.\$X.n}$ prediction error. If $X.n grows at a constant log-normal rate as in the Black Scholes Model, the predicted volatility growth estimate (StdDev($Y_{\Delta 3MR.Predict.n}$)) replaces the random walk volatility growth assumption (σ*sqrt(t)) in the Black Scholes Model.

The database has 650+ price responses at each horizon (1967:1 to 2023:12). Aggregating the realized responses into normalized histograms produces probability densities $\Delta P/P_{Data.n}$ at each horizon. The extracted Data moments have significant skewness and excess kurtosis. Moments extracted from normalized histograms aggregated from predicted responses $\Delta P/P_{Predict.n}$ have even larger excess kurtosis. Comparing the higher-order moments provides a sensitive test of the quality of the 3MR Reactive Price Model.

Another type of test uses plots to compare predicted price responses with realized S&P 500 responses at specific timesteps in the database. Because $Y_{\Delta 3MR.n}$ is linear in the shocks and the 3MRi risk variables are almost orthogonal, the plots also contain the price change attributable to each risk. The sum of the three responses forms the price response prediction for comparison with the S&P 500 price history.

The analysis emphasizes differentiating the adequacy of E/P vs. D/P to predict price histories. One study examines the extreme price changes during the 1987 boom/bust and the eight recessions in the database. Another study investigates the reasons behind the elevated equity prices during the late 1990s 'Internet Era.'

In the long horizon limit, investors lose all memory of previous yields and data, and $Y_{\Delta 3MR.n}$ evolves to become a static regression Y_{3MR} of the 3MRi on the sample mean <$X/P>. While the Y_{3MR} is not a discount model, it provides a statistically valid estimate of $X/$P_t$ at each point in time, like a discount model. Micro-founded consumption models Y_{MF} have time-varying structural parameters that provide economic explanations for valuation changes. Functionally connecting the 3MRi with the Y_{MF} parameters and requiring $Y_{3MR}=Y_{MF}$ offers a way to understand the sizeable explanatory power of the 3MRi risk variables.

The discount model studied here, $Y_{MF,}$ is closely related to the micro-founded consumption model studied by Campbell and Schiller (1987) in their classic paper describing their log-linear method. The Y_{MF} has three parameters: μ, γ and r_{rf}. Assuming the first order functional relationships, $r_{rf}=r_{rf}$(tcm1y), $\mu=\mu$($XGN) and $\gamma=\gamma$(cciN), the calibration results in an estimate for the risk aversion's mean $<\gamma> \sim 2.0$ and StdDev($\Delta\gamma$)/$<\gamma>$. Large values of γ are unnecessary when the driving risk variables are volatile.

Investors with short return horizons, where the return is based primarily on the price return, change the valuation by reacting directly to the 3MRi shocks.

The 3MR Reactive Price Model does not fit into any of the standard equity-related branches of the literature. It is much closer to the DSGE macroeconomic literature, where shocks

affect a macroeconomic model in its equilibrium state, and the analysis examines the return to the equilibrium state. In the 3MR Reactive Price Model, however, shocks to the 'state of risk' each month overshadow the return of the yield to its equilibrium state (<$X/P>), so the yield never remains in the equilibrium state.

The closest literature is the new literature that relaxes the rational expectations hypothesis, allowing belief-based expectations to serve as explanatory data variables in macrofinance models. Adam and Nagel's (2022) "Expectations Data in Asset Pricing" and Bordalo, Gennaioli, and Andrei Shleifer's (2022) "Overreaction and Diagnostic Expectations in Macroeconomics" provide in-depth reviews. This literature is strictly forward-looking.

Papers in this literature with relevance to this paper include Nagel and Xu (2022), "Asset Pricing with Fading Memory"; De La O and Myers (2002), "Subjective Cash Flows and Discount Rates; Bordalo et al. (2022) "Belief Overreaction and Stock Market Puzzles"; and De La O and Myers (2023) "Which Subjective Expectations Explain Asset Prices?"

Another literature relevant to this paper is the literature that studies connections between investor risk aversion extracted from option chains and changes in the real economy. Dew-Becker and Giglio's (2024) paper "Recent Developments in Financial Risk and the Real Economy" comprehensively reviews the current literature.

The remainder of this paper is organized as follows. Part 2 defines and estimates the Reactive Yield Model [$Y_{\Delta 3MR.n}$]. Part 3 studies the 3MR Reactive Price Model. Part 4 studies the significant price changes in 1987 and the database recessions. Part 5 explores 'why?' the 3MRi risk variables have such considerable explanatory power. Part 6 summarizes the findings.

2. The Reactive Yield Model

2.1. Reactive Regressions

The Reactive Yield Model posits the existence of a yield function having normalized data variables, Y(xiN$_t$,..) in its dataset, which returns an estimate \$X/P$_{Predict.t}$ for the yield datapoint \$X/P$_{Data.t}$. Applying Y(xiN$_t$..) to \$X$_t$ (where \$X$_t$ is either D or E), returns an estimate for the current price P$_t$=\$X$_t$/Y(xiN$_t$,..). A priori, Y's structure and data variables (xiN$_t$,…) are unknown. If Y(xiN,…) had a mathematical structure, a Taylor expansion calculates the first-order response of Y(xiN$_t$,…) to changes in its data variables.

Define a Taylor shock: $\Delta \text{xiN}_{\text{Taylor.n}} \equiv \text{xiN}_{\text{t+n}} - \text{xiN}_{\text{t}}$. where n is the monthly horizon. As in a mathematical Taylor expansion, the xiN data variables in the Taylor Shock remain perfectly autocorrelated as the horizon increases. The decline in the auto-correlation, ACF(xiN$_{t+n}$,xiN$_t$), is included by defining a generalized ('Full') data shock $\Delta \text{xiN}_{\text{Full.n}} \equiv \beta_{T.i.n}\text{xiN}_{\text{t+n}} - \beta_{O.i.n}\text{xiN}_{\text{t}}$ which includes separate regression coefficients for the shock's Origin (O) and Target (T) data variables. When the forward (Targeted) investor also loses memory of the Origin yield \$X/P$_t$, including a constant in the regression, a loss of memory of the shock's Origen value \$X/P$_t$ occurs. The Full Reactive Yield Model regression takes the form

$$Y_{\Delta \text{xiN.n}} \equiv lm\left(\frac{\$X}{P}_{t+n} \sim ß_{Const.n} + ß_{\frac{\$X}{P}.n}\frac{\$X}{P}_{t} + \Sigma\left(\beta_{T.i.n}\text{xiN}_{\text{t+n}} - \beta_{O.i.n}\text{xiN}_{\text{t}}\right)\right) \qquad (1)$$

As the horizon increases, ß$_{Const.n}$ increases while ß$_{\$X/P.n}$ decreases. These changes introduce a return-to-the-mean nudge into the Model. The Origin responses of the 3MRi, ß$_{O.i.n,}$ also decline relative to the Target responses ß$_{T.i.n.}$

There are two special cases.

1. The purely reactive (*Taylor*) limit: where $ß_{Const.n} = 0;\ ß_{\frac{\$X}{P}.n} = 1;\ \beta_{O.i.n} \neq 0$

$$Y_{\Delta \text{xiN.Taylor.n}} \equiv lm\left(\frac{\$X}{P}_{t+n} \sim \frac{\$X}{P}_{t} + \Sigma\, \beta_{Taylor.i.n}\,(\text{xiN}_{t+n} - \text{xiN}_{t})\right) \quad (2)$$

In this case, the investors do not use their knowledge of the equilibrium state.

2. The static limit: where and $ß_{Const.n} = 1.0;\ ß_{\frac{\$X}{P}.n} = 0;\ \beta_{O.i.n} = 0$

$$Y_{\text{xiN}} \equiv lm\left(\frac{\$X}{P}_{t} \sim <\frac{\$X}{P}> + \Sigma \beta_{xiN}(\text{xiN}_{t})\right) \quad (3)$$

In this case, the investor forgets the previous values of the Origen 3MRi risk variables and all X/P_{t-n,}$ and the Model becomes a regression of X/P_t$ on the 3MRi$_t$. Because the model uses normalized risk data variables (xiN), the regression constant is <$X/P>.

2.2. Identifying the 3MR Risk Variables

The estimation of the Reactive Yield Model requires the identification of the xiN variables. The search for the xiN used the static regression (Eq. 3). Given that the Model values the market portfolio, the search revealed that only variables pertinent to the whole economy exhibit high explanatory value. Ideal data variables have both high t-values and high mutual orthogonality. The analysis identified three classes of macro variables, commonly discussed as drivers of equity price changes in the financial press, as having both properties. The three classes, along with the specific data variables used in this paper, are:

1. A measure of the short risk-free rate (tcm1yN), the one-year treasury constant maturity yield.

2. A measure of trailing S&P 500 cash flow growth ($XGN), defined here as the year-over-year trailing growth rate $XG ≡ ($X(t)-$X(t-12))/$X(t-6).

3. A measure of *current* consumer confidence (cciN), here the Conference Board Consumer Confidence Index.

The Model collectively refers to these data variables as the “3 Macro Risks" because a change in any of them alters the yield, potentially decreasing the value of the investor’s portfolio. The 3MR triplet ≡ (3MR1=tcm1yN, 3MR2=$XGN, 3MR3=cciN). 3MRi identifies a member of the 3MR triplet.

Using the 3MRi, the static regression (Eq. 3) becomes

$$Y_{3MR.\$X} = \boldsymbol{lm}\left(\frac{\$X}{P} \sim < \frac{\$X}{P} > + \beta_{3\text{MR.tcm1yN}}\text{tcm1yN} + \beta_{3\text{MR.\$XGN}}\text{\$XGN} + \beta_{3\text{MR.cciN}}\text{cciN}\right) \quad (4)$$

Table 2.1 below displays the $Y_{3MR.\$X}$ regression statistics. The R^2 for both the E/P and D/P regressions exceed 60%. The last column shows the **Y**ield **I**mplied **P**rice **E**rror (YIPE) calculated from $YIPE \equiv 100 * \frac{\text{StdErr}(Y3\text{MR.\$X})}{\text{Mean}\left(\frac{\$X}{P}\right)}$. The pricing errors for both D/P and E/P exceed 20%, comparable to the size of the valuation errors found in the discount literature.

Table 2.2.1

$Y_{3MR.\$X}$ Regression Coefficients

$X/P	ßconst	ßtcm1yN	ß$XGN	ßcciN	R^2	StdErr(%)	YIPE(%)
E/P	6.8	1.8	0.70	-.95	0.65	1.51	22
t-value	117.6	31.15	11.94	-16.1			
D/P	2.8	0.97	0.11	-0.44	0.74	0.63	22
t-value	118.	40.37	4.62	17.9			

Table 2.1.2 displays the correlation matrix for the 3MRi risk variables. Although the correlations are not precisely zero, the model assumes correlations are low enough to allow predictions that assume the 3MRi are uncorrelated.

Table 2.2.2

3MRi Correlation Matrix

	tcm1yN	EGN	DGN	cciN
tcm1yN	1	-0.023	.087	-0.12
EGN		1	.13	0.19
DGN			1	.14
cciN				1

Table 2.2.3 shows the autocorrelation frequency (ACF) structure of the 3MRi risk variables. The column labeled ACF=12 reports the decline in the autocorrelation at a 12-month horizon. The column labeled hACF10% indicates the months required for the autocorrelation to decline to 10%. The differing ACF timescales of the 3MRi variables are the likely source for their quasi-orthogonality.

Table 2.2.3

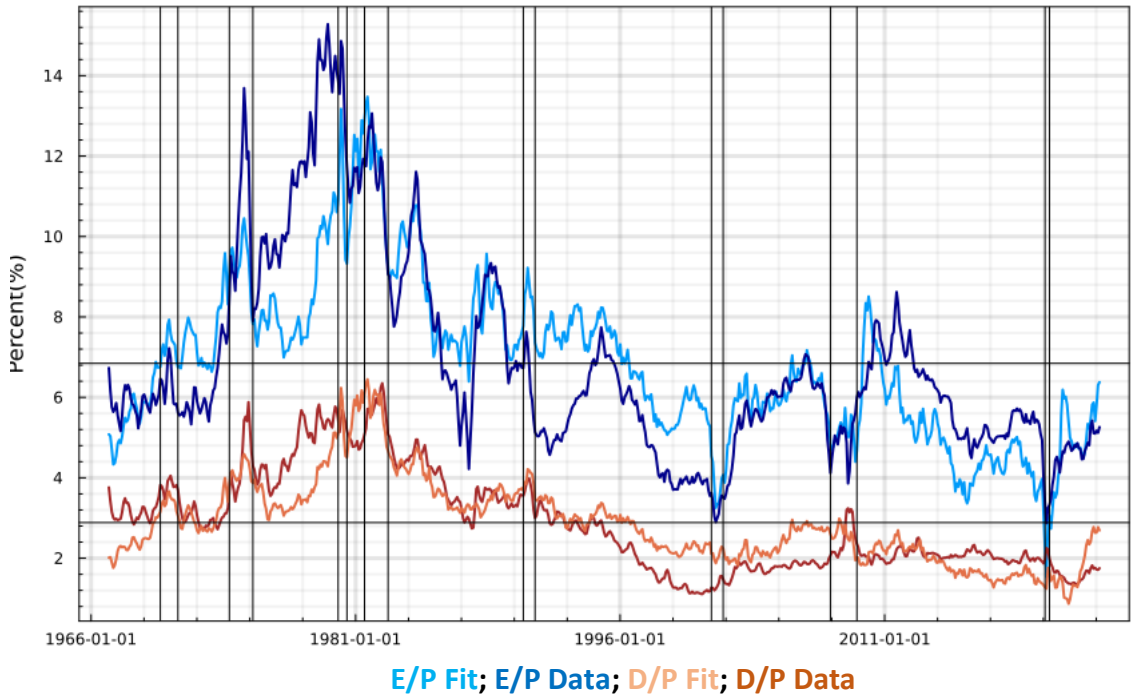
Auto Correlations

	ACF n=12	hACF10%
EGN	.001	11
DGN	.40	29
cciN	.63	27
tcm1yN	.84	150
(E/P) N	.82	96
(D/P) N	.90	155

Fig. 2.2.1 shows the fit of the $Y_{3MR.\$X}$ regressions to the $\$X/P_{Data}$. Note the significant serial errors.

Fig. 2.2.1

Fit to the Yield Data

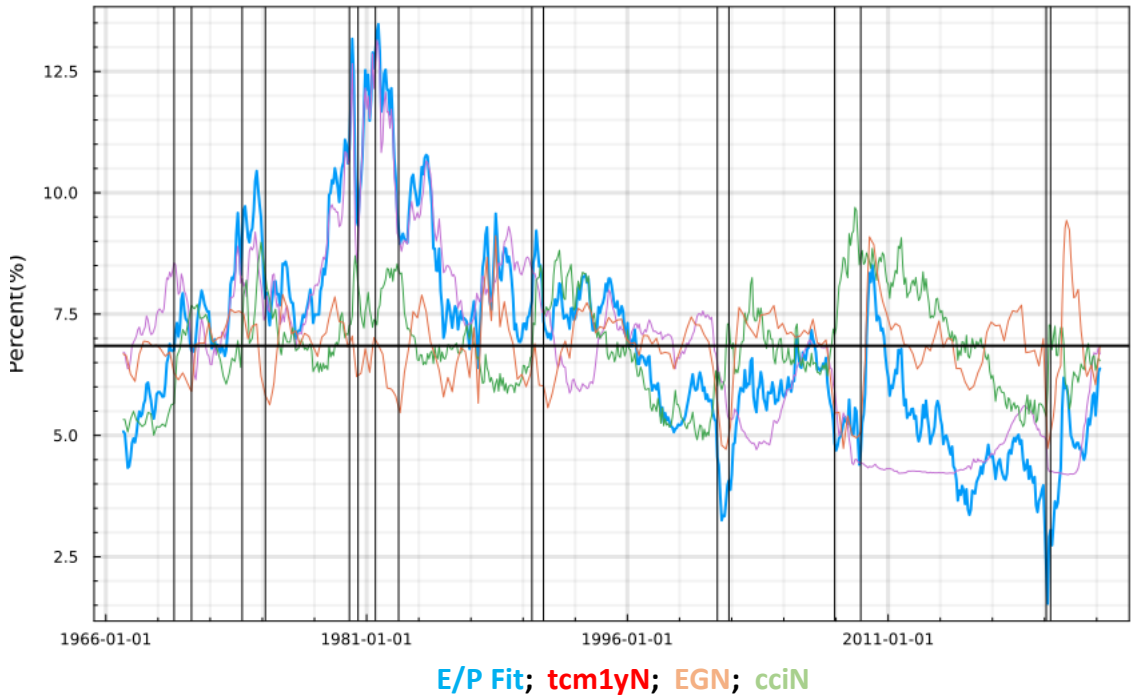


Note. The vertical black lines mark recession boundaries.

Because $Y_{3MR.\$X}$ is linear in the risk variables and the 3MRi are quasi-uncorrelated, Eq. 4 estimates the contribution from each risk variable to the StdDev($X/P). Fig. 2.2.2 shows the E/P decomposition. The long timescale factor (tcm1yN) broadly follows the high yields that occurred during the 1970s. The intermediate timescale factor (cciN) broadly follows business cycles. The short timescale factor EGN has an impact throughout the database.

Fig. 2.2.2.E

Decomposition of the E/P Fit



Note. The vertical black lines mark recession boundaries.

2.3. Estimating the Δ3MR Reactive Yield Model

Using the 3MRi risk variables, the Reactive Yield Model (Eq. 1) becomes:

$$Y_{\Delta 3MR.\$X.n} = \boldsymbol{lm}\left(\frac{\$X}{P}.\mathrm{n} \sim \beta_{const.n} + \beta_{\frac{\$X}{P}.0}\frac{\$\boldsymbol{X}}{\boldsymbol{P}}.0 + \Sigma\left(\beta_{(\Delta 3MRi.T).n}3MRi.n + \beta_{(\Delta 3MRi.O).n}3MRi.0\right)\right) \quad (5)$$

At each horizon (n), the Model estimates eight (8) regression coefficients. Table 2.3.1.E displays the regression statistics assuming $X=E. The row below each regressor displays its t-value. As the horizon increases, the absolute values of the Target regressors ßΔ3MRi.T.n increase, while the *absolute* value of the Origin regression coefficients (ßΔ3MRi.T.n) increase before starting to decline. The next two columns show the error statistics (the R^2 and the StdErr). The last column shows the reactive Yield Implied Price Error ($\Delta YIPE_{\Delta 3MR.E.n} \equiv StdErr(Y_{\Delta 3MR.E.n})/<\$X/P>$). At n=1, the

$\Delta YIPE_{\Delta 3MR.\ E.1}$ error is ~ 4%, more than a factor of five lower than static error: $YIPE_{3MR.\ E}$ ~ 22% (Table 2.2.1). For n=1, the $ß_{\Delta 3MRi.T.1} \cong (-1)^* ß_{\Delta 3MRi.O.1}$ (close to a Taylor shock).

Table 2.3.1.E

Regression Coefficients and Statistics of $Y_{\Delta 3MR.E.n}$

horizon	βconst	β(E/P).0	βtcm1y N.T	βtcm1y N.O	βEGN. T	βEGN. O	βcciN.T	βcciN.O	R^2	Std Err	ΔYIPE
1	0.12	0.98	0.74	-0.71	0.44	-0.38	-0.34	0.33	0.99	0.28	4.14
t-val	*2.29*	*133.47*	*7.91*	*-7.61*	*10.68*	*-9.18*	*-7.18*	*7.04*			
2	0.33	0.95	0.90	-0.83	0.46	-0.34	-0.47	0.43	0.97	0.46	6.73
t-val	3.93	79.28	9.62	-8.81	12.09	-8.61	-8.78	8.04			
3	0.53	0.92	1.00	-0.89	0.49	-0.30	-0.55	0.47	0.95	0.58	8.40
t-val	5.01	61.21	10.49	-9.28	13.42	-7.96	-9.70	8.36			
4	0.68	0.90	1.13	-0.99	0.51	-0.26	-0.61	0.50	0.94	0.64	9.37
t-val	5.76	53.37	11.91	-10.41	14.39	-7.21	-10.82	8.86	1		
5	0.82	0.88	1.28	-1.11	0.53	-0.23	-0.68	0.52	0.93	0.69	10.04
t-val	6.50	48.52	13.68	-11.87	15.11	-6.40	-11.98	9.27			
6	0.96	0.86	1.38	-1.19	0.55	-0.19	-0.73	0.53	0.92	0.73	10.60
t-val	7.17	44.77	15.14	-13.00	15.69	-5.49	-12.87	9.36			
7	1.11	0.83	1.42	-1.20	0.58	-0.16	-0.75	0.51	0.91	0.77	11.28
t-val	7.78	40.79	15.45	-13.04	15.89	-4.46	-12.88	8.72			
8	1.25	0.81	1.44	-1.19	0.61	-0.13	-0.76	0.49	0.90	0.81	11.87
t-val	8.29	37.54	15.26	-12.69	16.06	-3.48	-12.87	8.11			
9	1.36	0.80	1.41	-1.15	0.66	-0.09	-0.78	0.48	0.89	0.84	12.32
t-val	8.60	35.22	14.84	-12.17	16.45	-2.55	-13.23	7.90			
10	1.39	0.79	1.36	-1.10	0.73	-0.06	-0.83	0.51	0.89	0.85	12.45
t-val	8.63	34.46	14.56	-11.87	17.50	-1.60	-14.39	8.52			
11	1.40	0.79	1.32	-1.06	0.80	-0.02	-0.87	0.54	0.89	0.86	12.57
t-val	8.63	33.88	14.50	-11.74	18.34	-0.62	-15.54	9.19			
12	1.47	0.78	1.33	-1.06	0.83	0.00	-0.90	0.55	0.88	0.88	12.90
t-val	8.81	32.52	14.85	-11.90	18.35	0.12	-16.14	9.32			

Table 2.3.2 below shows the Taylor regression statistics for n=1.

Table 2.3.2
Regression Coefficients and Statistics for Taylor Case for n=1: $Y_{\Delta 3MR.E.Taylor.1}$

$X/P	ßconst	ßΔtcm1yN	ßΔ$XGN	ßΔcciN	R^2	StdErr(%)	YIPE(%)
E/P	.99	.78	.42	-.32	0.99	0.29	4.2
t-value	657	8.4	10.2	-6.9			
D/P	.99	.21	.06	-.15	0.99	0.13	4.3
t-value	651	8.4	10.2	-6.9			

The plots in Part 2.4 display the rest of the Taylor regression statistics and regression statistics for D/P regressions.

2.4. Analysis

2.4.1. Responses to Risk

Fig. 2.4.1 plots the evolution of the $\beta_{\Delta 3MRi.Full.\$X.(T/O).n}$ of the regression coefficients with increasing horizon. At each horizon (n), the model estimates eight (8) regression coefficients. As n increases, the $ß_{\Delta 3MRi.T.n}$, and the $-ß_{\Delta 3MRi.0.n}$ diverge as the memory of the Origin data variable declines. The solid horizontal lines indicate the $Y_{3MR.\$X}$ static regression coefficients $ß_{3MRi}$ shown in Table 2.1.1. As n->12, the $ß_{\Delta EGN.T.12}$ exceeds the static result $ß_{EGN}$. Note the significant differences in the separation rates among the three Origin regression coefficients $ß_{\Delta 3MRi.O.n}$, which arise from their differing autocorrelation frequencies. The plots also display the $ß_{\Delta 3MRi.\$X.Taylor.n}$ values. The Taylor ß(s) mainly lie between $ß_{\Delta 3MRi.T.n}$ and $ß_{\Delta 3MRi.O.n}$ values.

Fig. 2.4.1.E

Evolution of the Response Strengths: E/P

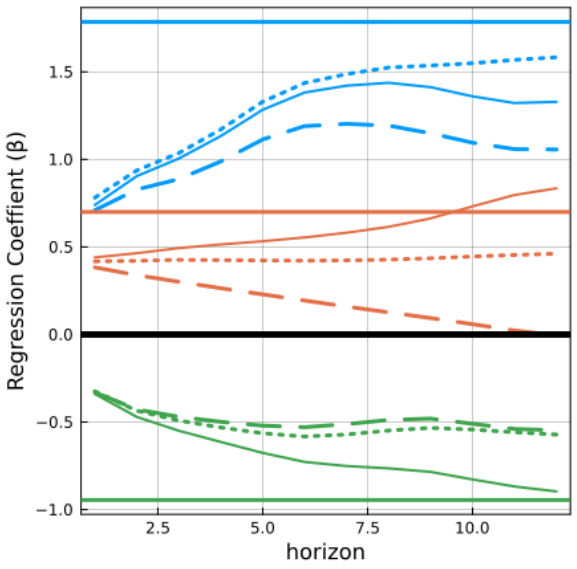
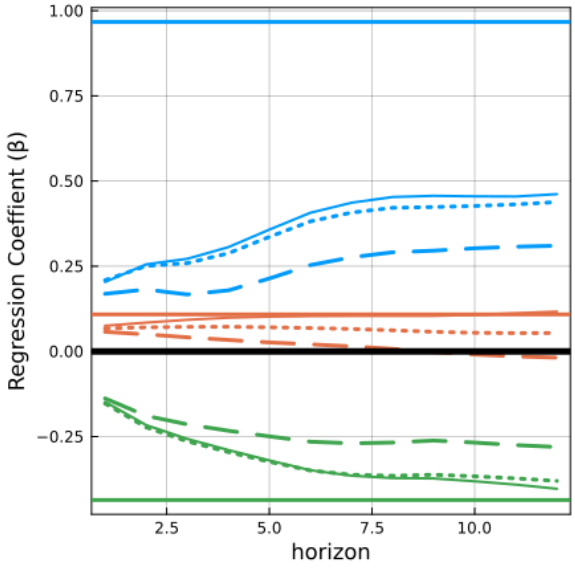


Fig. 2.4.1.D

Evolution of the Response Strengths: D/P



ß:tcm1yN.(O — , T— — , Taylor-- , Static —).n

ß:$XGN.(O — , T— — , Taylor-- , Static —).n

ß:cciN.(O — , T— — , Taylor-- , Static —).n

Note. See the text.

2.4.2. The Growth of Risk

Because the $\beta_{\Delta 3MRi.T.n}$ are the response to data values in the target investor's timestep, there is no memory loss of the $\beta_{\Delta 3MRi.T.n}$ by the targeted investor. Why do the $\beta_{\Delta 3MRi.T.n}$ increase with the horizon for identical normalized shocks (Δ3MRi.n)? Define the *amount of risk* as StdDev(Δ3MRi.n). Fig. 2.4.2 plots the *fraction* of the equilibrium risk, StdDev(Δ3MRi.n)/ StdDev(3MRi), expressed as the horizon increases. Because the 3MRi are normalized data variables, the StdDev(3MRi) = 1.0 (shown as the solid black line). Investors' exposure to increasing risk (StdDev(Δ3MRi.n)) explains the increase of $\beta_{\Delta 3MRi.T.n}$ with the horizon. The dashed lines plot sqrt(n)*($ß_{\Delta 3MR.T.n}/ß_{\Delta 3MR.T.1}$). The proximity of the paths creates an illusion of a Brownian Motion process. The solid black line plots the fractional increase of the yield StdDev(Δ($X/P).n).

Fig. 2.4.2
Fraction of Risk Expressed: E/P

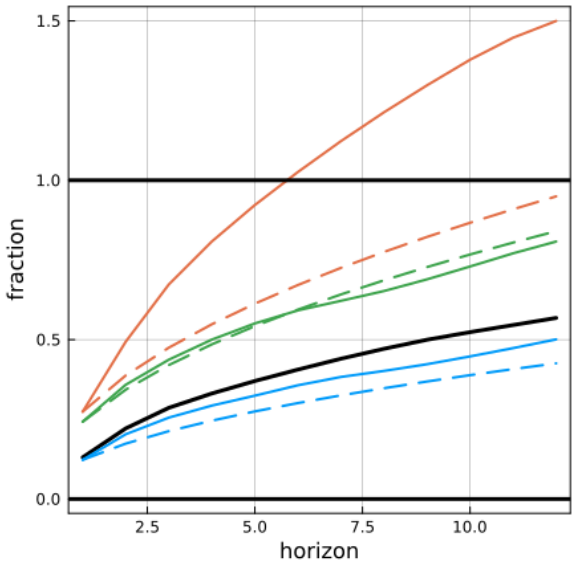
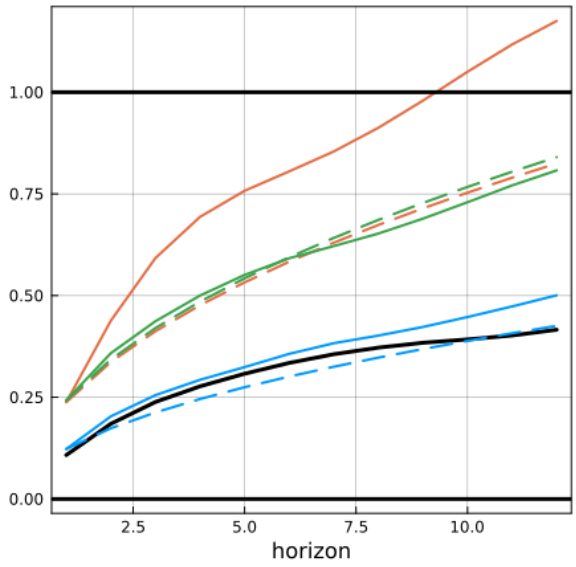


Fig. 2.4.2
Fraction of Risk Expressed: D/P



StdDev(Δtcm1yN.n) (fraction.n — ; sqrt(n)*fraction.1——)
StdDev(Δ$XGN.n) (fraction.n — ; sqrt(n)*fraction.1——)
StdDev(ΔcciN.n) (fraction.n — ; sqrt(n)*fraction.1——)
StdDev(Δ($X/P).n)

Note. See the main text.

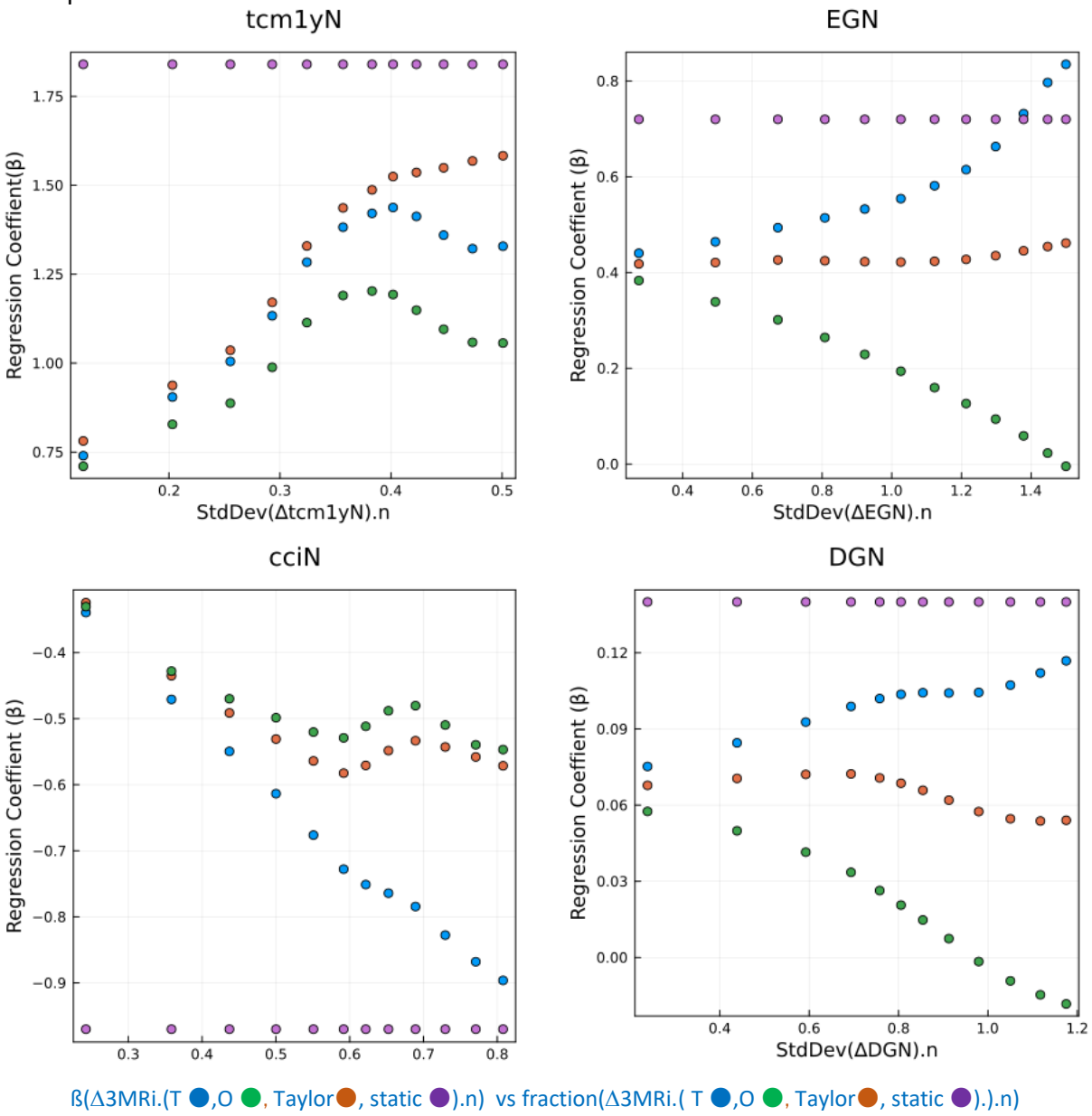
2.4.3. Response to Risk

Defining the Amount of Risk as StdDev(Δ3MRi.n) and the Response to Risk as $\beta_{\Delta 3MRi.(T/O).n}$, Figures 2.4.3.a,b,c,d below plot the Response to Risk vs the Amount of Risk for each 3MRi variable. The plots show the negative responses of the Origin risks to facilitate observation of the decline of the Origen response. The Target Response is largely linear in the risk up to horizons n=6. The Responses of the Origin risk variables depend on their autocorrelation frequency (ACF). For $\beta_{\Delta tcm1yN.O.n,}$ where the acf10% ~ 150 months, the response declines slowly relative to the Target Response increase. At the other extreme, the rapidly declining autocorrelation of $\beta_{\Delta EGN.O.n}$ results in an almost linear decline in its response. At horizons starting at n=6, both $\beta_{\Delta tcm1yN.(T/O).n}$ Responses begin to saturate, while for the $\beta_{\Delta cciN.(T/O).n}$ pair, the $\beta_{\Delta cciN.O.n}$ Response shows an unknown structure.

Summarizing the Target Risks, for n~6, the hypothesis that the response is proportional to the risk holds. For n > 6, $\beta_{\Delta tcm1yN.T.n}$ saturates, $\beta_{\Delta cciN.T.n}$ continues its linear descent while $\beta_{\Delta EGN.T.n}$ becomes more significant than its static limit, StdDev(EGN). The responses of the Origin risk variables depend on their autocorrelation frequencies on all horizons.

Fig. 2.4.3.a,b,c,d

Response to Unit of Risk



Note. See the main text.

2.2.4 Fading Memory

Why does the ßΔ3MRi.O.n decline relative to the ßΔ3MRi.T.n with increasing horizon? To determine if the decline is due to decreasing autocorrelation, Figure 2.4.4 compares the decline in the ACF(3MRi.n,3MRi.0) with increasing horizon to the decline in the ratio ß3MRi.O.1/ß3MRi.O.n with the horizon. The declines in ß3MRi.E.O.1/ß3MRi.E.O.n closely follows the decline in the

ACF(3MRi.n,3MRi.0) declines. One can interpret this decline as an investor's 'fading memory' of the Origin risk variable with the increasing horizon. For $X=D, the ratio ßDGN.O.1/ßDGN.O.n declines much faster than the autocorrelation, indicating a misspecification in the $Y_{\Delta 3MR.\$X.n}$ Model when applied to D/P.

Fig. 2.4.4.E
Loss of memory E/P

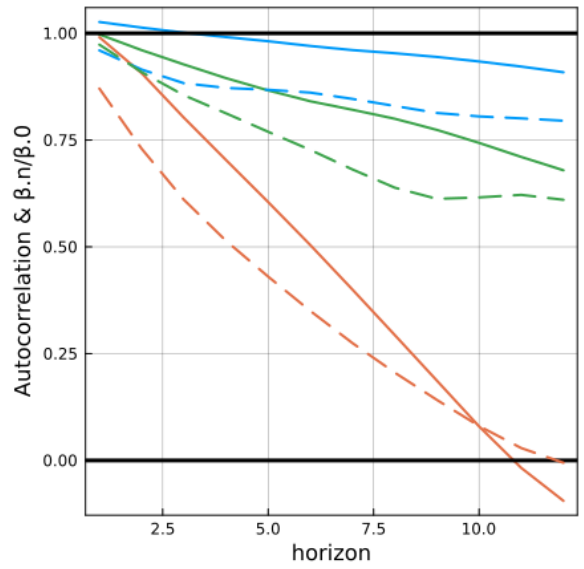
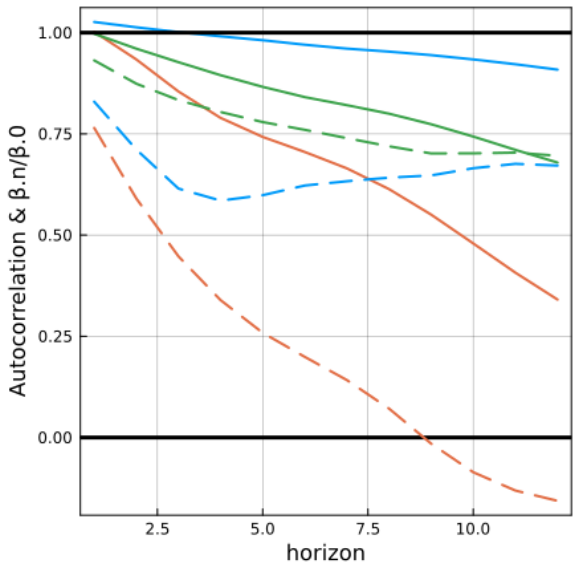


Fig. 2.4.2
Loss of memory D/P



acf(tcm1yN.n, tcm1yN.0) — ; ß(tcm1yN.T.n)/ ß(tcm1yN.T.1) ----
acf($XGN.n, $XGN.0) — ; ß($XGN.T.n)/ ß($XGN.T.1)-----
acf(cciN.n, cciN.0). — ; ß(cciN.T.n)/ ß(cciN.T.1)----

Note. See the main text.

2.4.5 Return to the Mean

Suppose that at time t, X/P_t$≠<$X/P>. Fig. 2.4.5 shows how, in the absence of shocks (3MRi$_{t+n}$ = 3MRi$_t$), $X/P.n evolves toward its equilibrium value <$X/P>. The evolution of ßConst.n and ß$X/P.O.n determine the path of $X/P.n to its equilibrium value (see Table 2.3.1 for the $X=E case). As the horizon increases, ßConst.n increases, while ß$X/P.O.n decreases, causing $X/P to evolve toward its equilibrium state <$X/P>. However, in practice, X/P_{t+n}$ never returns to equilibrium

because the yield receives new monthly shocks. The return-to-the-mean effect becomes increasingly significant as Abs($X/P - <$X/P>) increases.

Fig. 2.4.5.E

Return to the Mean E/P

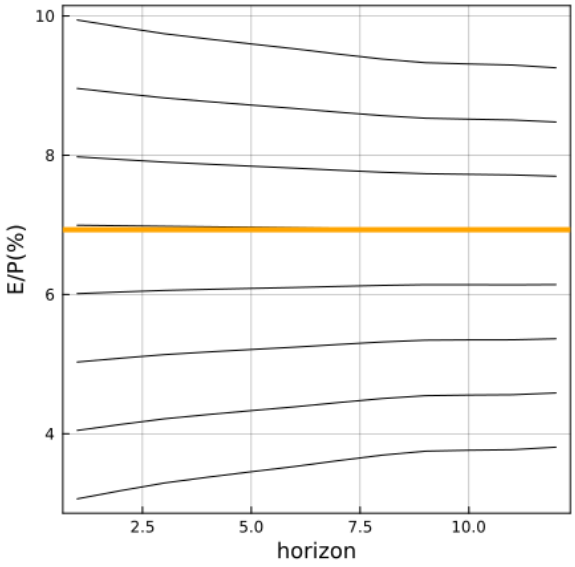
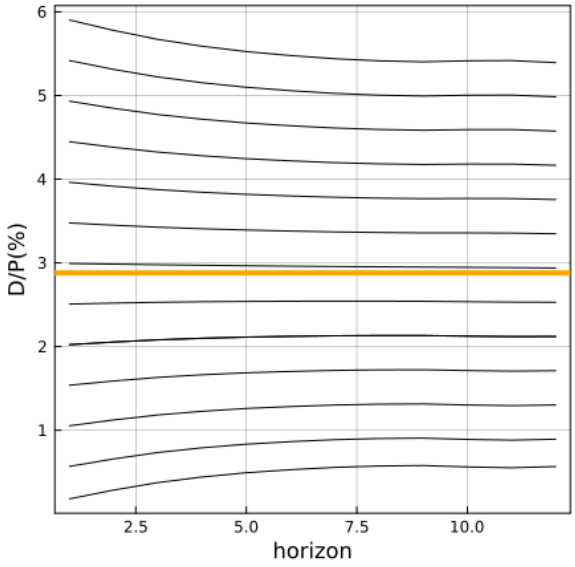


Fig. 2.4.5.D

Fig. 2.4.5.D Return to the Mean D/P



$X/P.n=ßConst.n + ß$X/P.O.n*$X/P.0 —

Note. The horizon Lines (—) identify <$X/P>

2.4.6 Error Growth

Suppose an investor has perfect foresight for Δ$X.n and the Δ3MRi.n. Since investors in the Reactive Yield Model know $X.n with certainty, the price error for $P_{\Delta 3MR.n}$ is determined by the prediction error of the $Y_{\Delta 3MRi.n}$ regression. An estimate for the price error is the Yield Implied Price Error $\Delta YIPE_{.\$X.n} \equiv StdErr(Y_{\Delta 3MR.\$X.n})/<\$X/P>$ shown for $X=E in the last column of regression Table 2.3.1.E.

Fig. 2.4.6 shows the yield prediction error using five different calculation methods.

1. The horizontal line labeled ‘static’ shows the $YIPE_{3MR}$ static error (Table 2.1). In the static case, the investor has exposure to the entire variance of $X/P.

2. The line labeled ‘Const.$_{\$X/P.0}$ ’ shows the error if $X/P.n = $X/P.0. For both D and E, the error becomes comparable to the $YIPE_{3MR}$ error as n ->12.

3. The line labeled 'Taylor' plots the ΔYIPE.Taylor.n error.

4. The line labeled 'Full' plots the ΔYIPE.Full.n (Table 2.3.1, last column).

5. The line labeled √n*ΔYIPE.Full.1 shows the Brownian error growth starting at n=1in the Full Model.

At low horizons, the Const.$X/P.0 case exhibits a significant error reduction compared to the static error case. Further error reduction depends on the accuracy of the $X/P.n predictions. The Full and Taylor ΔYIPE errors grow more rapidly than √n at small horizons, but the growth slows and saturates as n ->12. The error for $X=E saturates more slowly than the Taylor error because the memory effect becomes more significant as the horizon increases. The long horizon ΔYIPE.D.n error is greater than that of the E/P Model error at all horizons.

Fig. 2.4.6.E
ErrorGrowth: $X=E

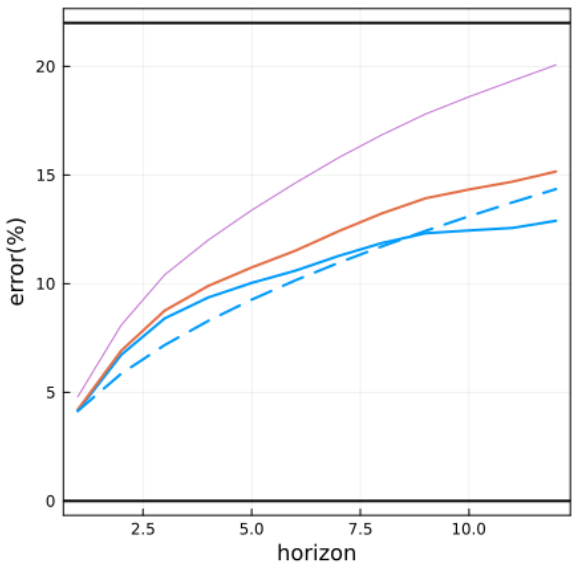
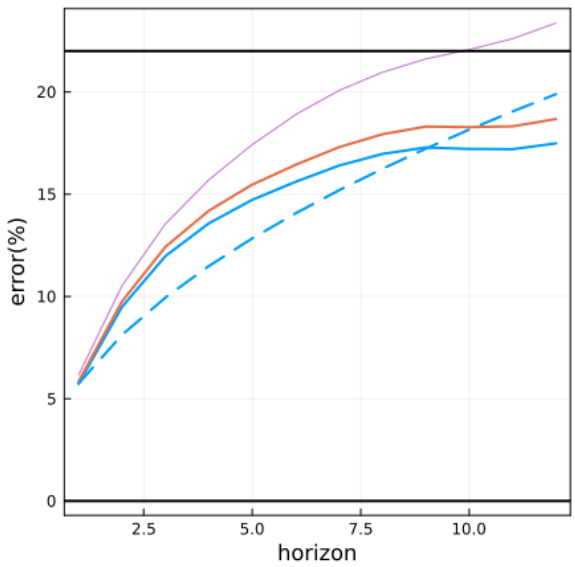


Fig. 2.4.6.E
ErrorGrowth: $X=D



YIPE3MR —; Const.$X/P.0 —; ΔYIPE.Taylor.n —; ΔYIPE.Full.n —; $\sqrt{n}$*ΔYIPE.Full.1 ——

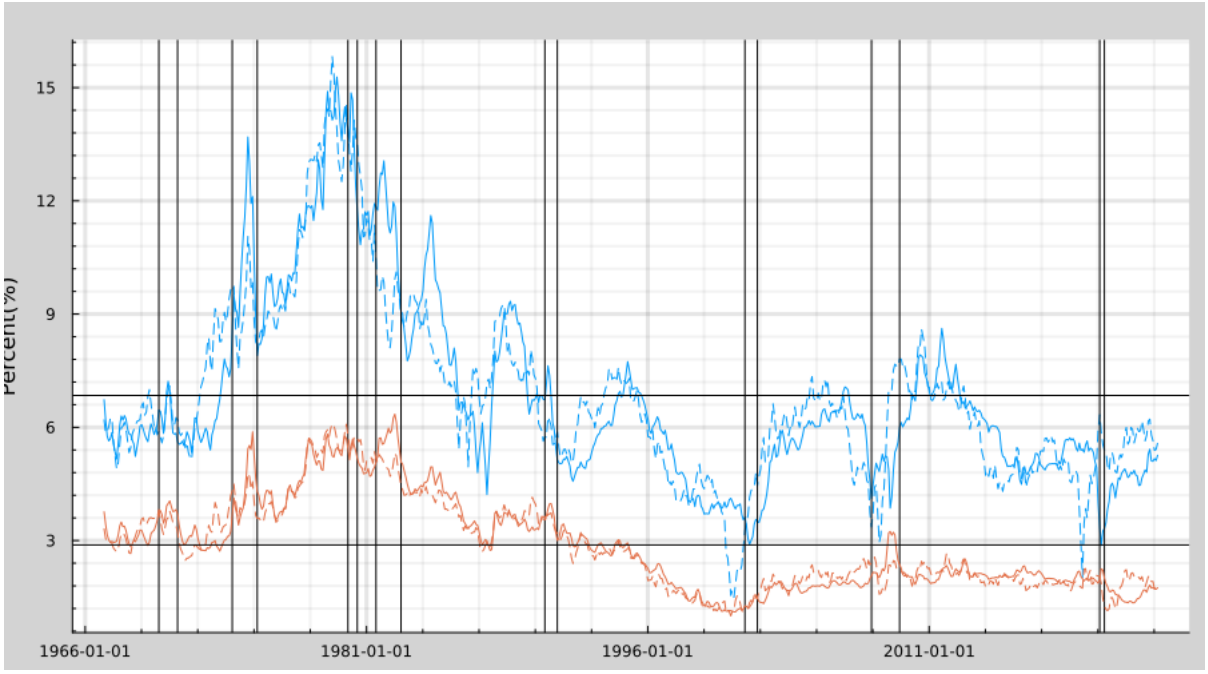
Note. See the main text.

2.4.7 Fit to the Data

Fig. 2.4.7 plots the $Y_{\Delta 3MR.\$X.t+6}$ predictions for comparison with the six-month forward data $\$X/P_{Data.t+6}$. The improvement in the fit compared to the static model fit $Y_{3MR.\$X}$ (Fig. 2.2.1) is apparent.

Fig. 2.4.7

Six-month Forecast: Fit to Data



E/P.t+6 Fit; E/P Data.t+6; D/P Fit.t+6; D/P Data.t+6

Note: Vertical lines mark recession boundaries.

3. The 3MR Reactive Price Model

An investor at time t, who has expectations for the values of $\$X_{t+n}$ and the $3MRi_{t+n}$ risk variables, can estimate P_{t+n} by calculating how the Targeted investor at time t+n will set the price if the investor reacts to a shock that originated at time t (the shock's Origin timestep). The 3MR Reactive Price Model applies the yield prediction $Y_{\Delta 3MR.\$X.n}$ to $X.n to calculate the price.

$$P_{\Delta 3MR.\$X.n} = \frac{\$X.n}{Y_{\Delta 3MR.\{Full\ or\ Taylor\}.\$X.n}} \tag{4}$$

3.1 Reactive Equity Pricing

If the Targeted investor is in the current time step t_0, the investor receives a data report whose Origin is in a previous timestep. In principle, the investor could look back to any past timestep. However, because the Yield Implied Price Error (ΔYIPE.n) error increases with the horizon (see Fig 2.4.6), the optimum choice for the investor is to look back only to the previous timestep (t_0-1) because ΔYIPE.1 ~ 4.2% while ΔYIPE.2 ~ 6.9% (see Table 2.3.1). The asynchronous reports of the $3MRi_t$ shocks help explain the sizeable intramonthly price volatility. Since the financial press widely discusses the 3MRi risk variables as drivers of equity price change, there should be no issue of 'Risk Factor Relevance' (Chinco et al., 2022).

The Reactive Yield Model has no intertemporal concept of "properly anticipated" as in Samuelson (1965). The reports of the 3MRi risk variables provide new information that previous timesteps have not integrated into the price. If investors anticipate the report of a $3MRi_t$ risk variable in the current time step and change the price before the report, the report of the $3MRi_t$ does not affect the price. If investors do not anticipate the $3MRi_t$ report in the current times step, the price changes after the $3MRi_t$ report. Either way, the Δ3MR Yield Model always imputes the shock $\Delta 3MRi_{t-1->t}$ into $\$X/P_t$ into the price in the current timestep (t) price.

Table 2.3.2 displays the regression statistics for n=1 Taylor shocks. The t-values for the n=1 shocks are all statistically significant, exceeding 6.9. The $\Delta YIPE_{.1.E} \approx 4.2\%$ is slightly less than $StdDev(\Delta P/P_{Data.1}) \approx 4.5\%$.

When the investor who receives the shock is in a future time step, the investor in the current time step can estimate how a future investor would set the yield as the reactive response to shocks whose Origen is in the current timestep, using the investor's expectations for the risk variables. As

the horizon increases, the future investor must look further and further back in time, so the prediction error increases with horizon.

3.2. Physical Densities: The Illusion of Randomness

The yield history $X/$P_t$ results from the monthly price changes $\Delta\$X/P_{t+n-1->t+n}$. The $Y_{\Delta 3MR.n}$ prediction does not require path information, so the price response ($\Delta P/P_{Data.n.t}$) can be aggregated directly into a normalized histogram at each horizon. For the market portfolio (the S&P 500), the issue is how to grain the distribution when there are only a limited number of instances to aggregate because the database studied extends only one or two decades backward. Here, the database extends back to the mid-1960s, so there are more than 650+ instances to aggregate at each horizon, making finer graining possible.

Figure 3.2.1 displays $\Delta P/P_{Data.n.t}$ normalized histograms (blue) for n=1,6,12 obtained by aggregating the price changes into normalized histograms. The vertical blue lines indicate the Mean($\Delta P/P_{Data.n}$), the ±1.0 StdDev($\Delta P/P_{Data.n}$), and the ±2.0 StdDev($\Delta P/P_{Data.n}$). The large amount of data beyond ±2.0 StdDev($\Delta P/P_{Data.n}$) markers in the $\Delta P/P_{Data.1}$ histogram indicates high excess kurtosis. The excess kurtosis decreases with the horizon and almost disappears in the $\Delta P/P_{Data.12}$ density. In the $\Delta P/P_{Data.12}$ case, the asymmetry toward negative values indicates skewness in the Data. The Data densities are largely consistent with the risk-neutral densities extracted from S&P 500 option chains.

Fig. 3.2.1 also plots normalized histograms (orange) aggregated from the $\Delta P/P_{\Delta 3MR.Taylor.n.t}$ predictions. The aggregations closely follow the Data aggregations. The diffusive appearance is not the result of a random process; it is the result of the response of the equity yield to asynchronous changes in the three stationary 3MRi risk variables with differing autocorrelation frequencies.

Fig.3.2.1.a

ΔP/P.1 Densities: Full Model

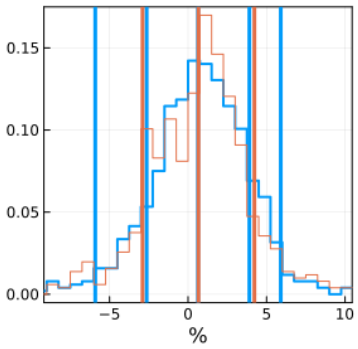


Fig.3.2.1.b

ΔP/P.6 Densities: Full Model

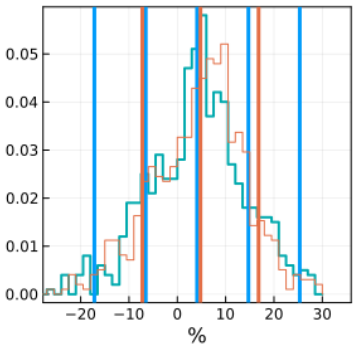
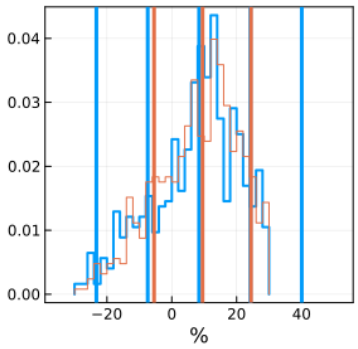


Fig.3.2.1.c

ΔP/P.12 Densities: Full Model



$\Delta P/P_{Data.n}$ --- $\Delta P/P_{\Delta 3MR.n}$ ---

Note: Comparison of Data and Predicted Densities

A more sensitive test of the Δ3MR Model compares the moments of the Data density with the moments of the Predicted density. Fig. 3.2.2.a,b compares the moments (*M*) of $\Delta P/P_{Data.(Mean,StdDev,Skewness,Kurtosis).n}$ with the predicted moments of $\Delta P/P_{\Delta 3MR.(Mean,StdDev,Skewness,Kurtosis).n}$. The Data density moments resemble the moments extracted from the S&P 500 option chains, excess kurtosis at n=1, which decreases with the horizon, and negative skewness, which becomes smaller with the increasing horizon. If the model made predictions without error, the moments of the predicted density would be the same as the Data moments. Differences in the moments provide insights into the source of the errors.

Analysis of the Moments.

1. *Mean*: The $M_{Data.Mean.n}$ moment is almost linear with the horizon. Both the $M_{\Delta 3MR.(Full,Taylor).Mean.n}$ moments closely follow $M_{Data.Mean.n}$.
2. *Volatility*: The $M_{Data.Volatility.n}$ moment increases more rapidly than sqrt(n) at low horizons. Both the $M_{\Delta 3MR.(Full,Taylor).Volatility.n}$ moments grow faster than the $M_{Data.Volatility.n}$ moment at low horizons. At horizons beyond n=6, both the $M_{\Delta 3MR.(Full,Taylor).Volatility.n}$ moment's growths begin to saturate. The saturation occurs because the $Y_{\Delta 3MR.n}$ prediction cannot exceed the database yield volatility (StdDev($X/$P_{Data}$)).

3. *Skewness*: The $M_{\text{Data.Skewness.n}}$ moment is slightly negative at n=1 and becomes less negative with increasing horizon. The $M_{\Delta 3MR.(\text{Taylor}).\text{Skewness.n}}$ moment shows almost no skewness, while the $M_{\Delta 3MR.(\text{Full}).\text{Skewness.n}}$ moment has positive skewness at low horizons.
4. *Excess Kurtosis*: The $M_{\text{Data.ExcessKurtosis.n}}$ moment is significant at low horizons but gradually declines with increasing horizon. The $M_{\Delta 3MR.(\text{Full,Taylor}).\text{ExcessKurtosis.n}}$ moments significantly exceed the $M_{\text{Data.ExcessKurtosis.n}}$ moment at low horizons and then decline when the horizon exceeds n=6. The Predicted Excess Kurtosis increases more than the Data Excess Kurtosis because when the prediction regression targets the outliers in the Data Density, the prediction error further increases the number of outliers in the prediction density.

Fig. 3.2.2.a
Prediction Moments: Full Model

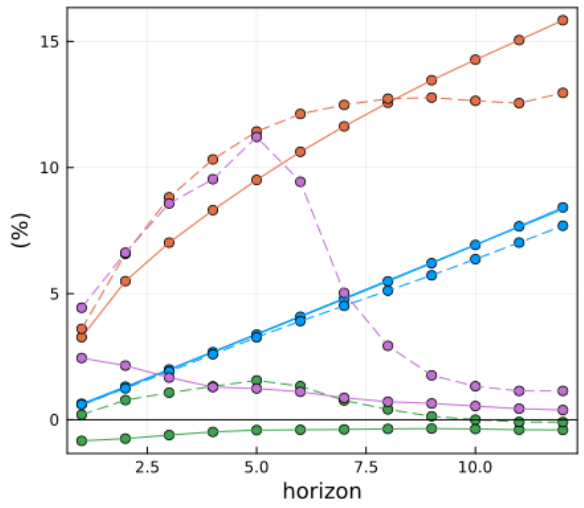
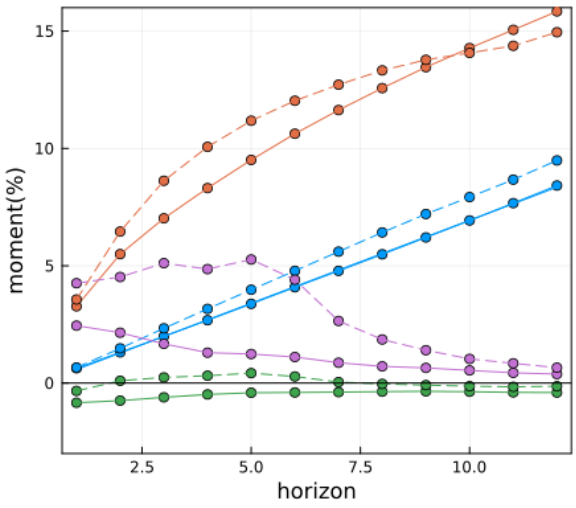


Fig. 3.2.2.b
Prediction Moments: Taylor Model



Mean StdDev Skewness Kurtosis
M_{Data}:---- $M_{\Delta 3MR}$:----

Note. See the main text.

3.3 Price Prediction Errors

Fig. 2.4.6 plots the Yield Implied Price Errors $\Delta\text{YIPE}_{\Delta 3MR.\$X.n} \equiv \text{StdErr}(Y_{\Delta 3MR.\$X.n})/\langle \$X/P \rangle$. The division by <$X/P> is an approximation that works when all the price prediction error resides in

the yield prediction. Here, studies of the prediction errors generated by the 3MR Reactive Price Model eliminate the approximation.

Define $\Delta P/P_{\Delta 3MR.Error.n} \equiv 100*(P_{\Delta 3MR.t+n} - P_{Data.t+n})/P_{Data.t}$. Fig. 3.3.1.a,b,c plot the $\Delta P/P_{\Delta 3MR.Taylor.error.n}$ densities for n=1, 6, and 12 constructed using the same methodology used to construct the $\Delta P/P_{\Delta 3MR.Predict.n}$ densities. The plots also include a fitted normal distribution.

Fig.3.3.1.a

Error Densities: Taylor Model n=1

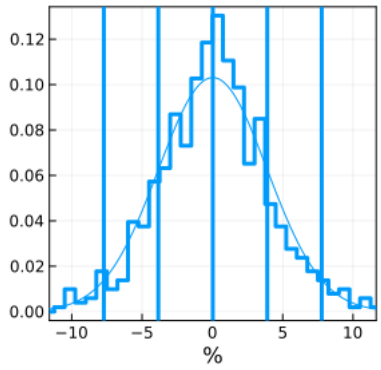


Fig.3.3.1.b

Error Densities: Taylor Model: n=6

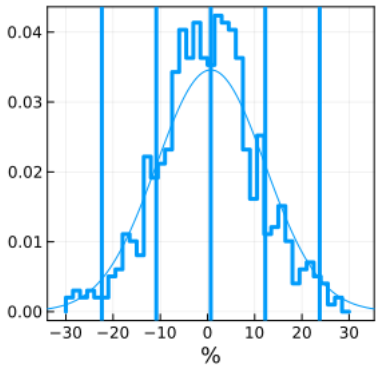
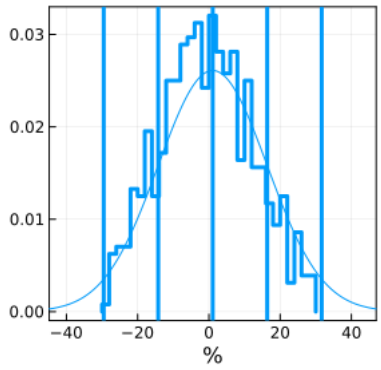


Fig.3.3.1.c

Error Densities Taylor Model: n=12



$\Delta P/P_{\Delta 3MR.Error.n}$ --- Fit of Normal Distribution --

Note. See the main text.

Fig. 3.3.2.a,b shows the $M_{\Delta 3MR.(Taylor,Full).Error.n}$ error density moments. The $M_{\Delta 3MR.(Taylor,Full).Error.Mean.n}$ and $M_{\Delta 3MR.(Taylor,Full).Error.Skewness.n}$ moments are small for both Models. Both $M_{\Delta 3MR.(Taylor,Full).Error.ExcessKutosis.n}$ moments are significant and peak around n=5. This pattern resembles the peaking of Excess Kurtosis found in the $\Delta P/P_{\Delta 3MR.Predict.n}$ moments (Fig.3.2.2). The $\Delta YIPE_{.\$X.n}$ error estimates (Fig. 2.4.6.E) are close to $M_{\Delta 3MR.(Taylor,Full).Error.\ Volatility.n}$ moments in both the Full and Taylor Models. There is quasi-equality between the $M_{\Delta 3MR.(Full,Taylor).Predict.Volatility.n}$ moments (Fig. 3.3.2) and the $M_{\Delta 3MR.(Full,Taylor).Error.Volatility.n}$ moments. Additional error reduction remains an issue for future research.

Fig. 3.3.2.a
Errors: Full Model

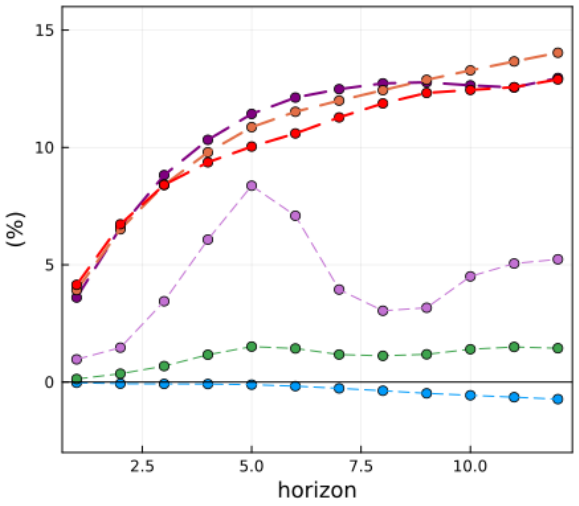
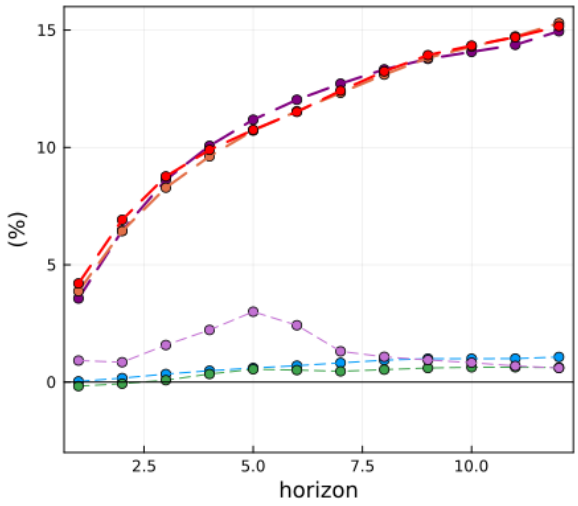


Fig. 3.3.2.b
Errors: Taylor Model



Error Moments: Mean StdDev Skewness Kurtosis
ΔYIPE errors, Predicted Volatility Moment

Note. Predicted Volatility Moments are from Fig. 3.2.2.a.b

4. Price Response Studies

4.1. Yield Response Decompositions

Figure 2.2.1 shows the decomposition of the $Y_{3MR.Predict.\$X.n}$ prediction in the static limit into the contributions from each 3MRi risk. Equation Set 4.1 shows the decomposition of $Y_{\Delta 3MR.\$X.n}$ reactive response. The Base case (Eq. 4.a) exhibits the regression coefficients (ß). The regression coefficients (ß) are inferred from the context of the other decomposition equations.

Eq. Set 5.a,b,c,d,e Decompositions of the Responses to Δ3MRi Macro Shocks

$$(5.a)\ \ Base\text{: } Y_{\Delta 3MR.\$X.Base.n} \qquad \left(\frac{\$X}{P}.\mathrm{n} = ß_{Const} * 1 + ß_{\frac{\$X}{P}.0} * \frac{\$X}{P}.0\right)$$

$$(5.b)\ \ tcm1yN\text{: } Y_{\Delta 3MR.\$X.tcm1yN.n} \left(\frac{\$X}{P}.\mathrm{n} = 1 + \frac{\$X}{P}.0 + tcm1yN.n + tcm1yN.0\right)$$

$$(5.c)\ \ \$XGN\text{: } Y_{\Delta 3MR.\$X.\$XGN.n} \qquad \left(\frac{\$X}{P}.\mathrm{n} = 1 + \frac{\$X}{P}.0 + \$XGN.n + E\$XGN.0\right)$$

$$(5.d)\ cciN\text{: } Y_{\Delta 3MR.\$X.cciN.n} \qquad \left(\frac{\$X}{P}.\mathrm{n} = 1 + \frac{\$X}{P}.0 + cciN.n + cciN.0\right)$$

$$(5.e)\quad Full{:}\ Y_{\Delta 3MR.\$X.Full.n} \qquad \left(\frac{\$X}{P}.\mathrm{n} = 1 + \frac{\$\boldsymbol{X}}{\boldsymbol{P}}.0 + tcm1yN.n + tcm1yN.0 + \$XGN.n + \$XGN.0 + cciN.n + cciN.0\right)$$

4.2. Price Response Plots

Price response plots compare the predictions of the 3MR Reactive Price Model with the price history of the S&P 500. Equations 5.a-e calculate the price response decomposition. The plots display E/P and D/P predictions side-by-side to facilitate easy comparison. Fig. 4.2.1 plots the 3MR Reactive Price Model prediction for the 'soft landing' that occurred in CY 1994. The vertical line marks the forecast month (Dec. 1993), and the solid horizontal line marks the Dec. 1993 risk-adjusted average price. The horizontal dashed lines indicate the percent price change ΔP/P(%) in increments of ± 10%.

Fig. 4.2.1.E
1993: E/P

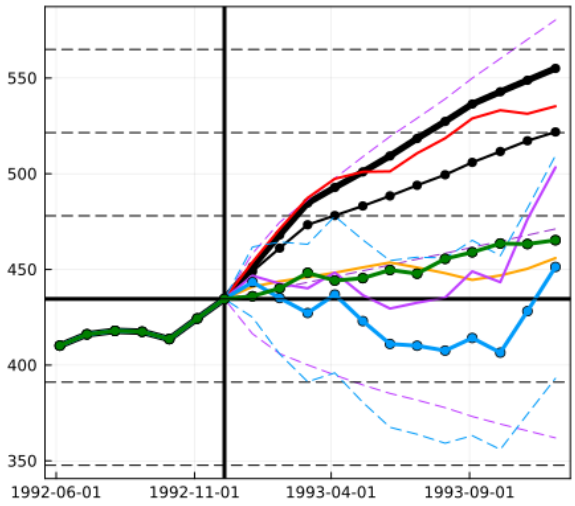
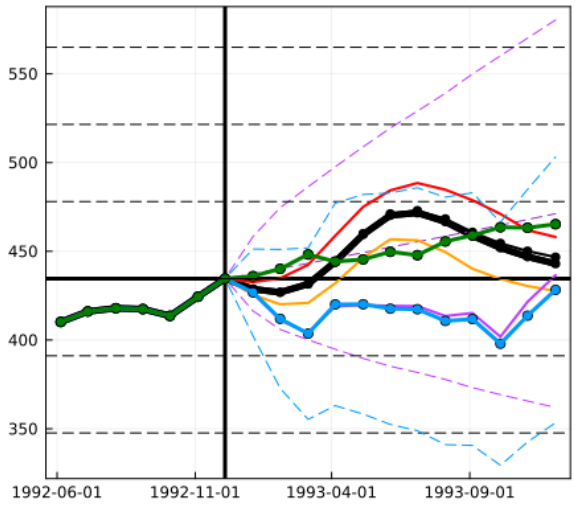


Fig. 4.2.1.D
1993: D/P



Variance Bounds: Mean.n; StdDevP.n; StdDevM.n ----; **Basic Data:** sp500.n -●-●-; **Const($X/P).n** ——

Valuation Adjust: Base.n-●-●-; ΔtcmlyN.n ——; ΔSXGN.n ——; ΔcciN.n —— **Prediction:** Full.n-●-●-; StdErr.n----

Note. See the explanations below.

Each plot contains four categories of lines. There are several lines within each category, each with its own label. The analysis concentrates on the E/P Model.

A. Price Variance Boundaries:

1. The set of lines labeled **Mean.n, StdDevP.n, and StdDevM.n** — show the evolution of the ΔP.n dispersion with the horizon.

B. Basic Data:

2. The line labeled **sp500.n** shows the S&P 500 price trajectory.

3. The solid line **Const($X/P.n)** line shows how the price would have evolved if the valuation did not change with the horizon, meaning $X/P.n = $X/P.0 for n in 1:12. The price then follows the cash flow ($X.n). The difference between the sp500 and Const($X/P) lines is the amount the price changed due to a change in the yield. In this case, the divergence was significantly different when $X=E.

C. Valuation adjustments:

4. "The line labeled **Base.n-●-●-** uses Eq. 5.a shows how the price would have evolved toward the equilibrium value <$X/P> if there were no shocks to the risk variables. In this case, there is only a small difference between the **Base.n** and the **Const($X/P.n)** lines because $X/P.0 ~ <$X/P>.

5. & 6. & 7. "The lines labeled **Δtcm1yN.n----; Δ$XGN.n----; ΔcciN.n----** show the price response decomposition (Eq. Set 5.b, 5.c), the amount the price would have responded relative to the **Base.n** if only one of the risks was present. In this case, there were large negative deviations from the **Base.n** in the **ΔcciN.n** and **Δ$EGN.n** responses.

D. Predictions:

8. "The line labeled **Full.n-●-●-** calculated using Eq. 5.e, aggregates the responses from the 3MRi shocks to form the predicted response which is to be compared with the **sp500** price history. In this case, the negative responses from **ΔcciN.n** and **Δ$EGN.n** resulted in a slightly negative price growth path, despite the significant earnings growth in CY 1994, in agreement with the flattish **sp500** price growth in Cy1993.

9. The two lines labeled **StdErr — —** show the ΔYIPE.$X.n StdErr error growth estimates shown in Fig. 2.4.6. The large standard errors make choosing between the E/P and D/P difficult.

4.3 Studies

Are markets efficient? Are investors rational? Many scholars cite the soaring prices in 1987 and the late 1990s as proof of investor irrationality. Malkiel (2003) disputes the irrationality hypothesis. The decline in prices during recessions is also difficult to explain within the rational expectations paradigm. This paper studies these periods to see how well the 3MR Reactive Price Model explains the price changes, concentrating on which yield ratio (D/P vs E/P) investors choose as their valuation ratio. The displays show the E/P and D/P plots side-by-side to simplify

comparison. The reader should analyze the plots using the methodology outlined above. The text box below the plots contains an analysis of the quality of the fits.

4.3.1 CY1987

In early 1987, corporate earnings began a growth spurt, rising 70% by September 1987. The S&P 500 rose 30% by September, but the price growth then reversed, and prices declined to levels comparable to those at the beginning of 1987. Fig. 4.3.1 shows the fit to the data.

The sp500 price response (**sp500.n)** was significant, almost doubling **StdDevP.n** by Sept. 1987. The D/P Model **Const(D/P).n** growth was small (~ 8%), setting the foundation for only a modest price increase. The **Const(E/P.n)** growth, on the other hand, reached almost 2.0* **StdDevP.n** by Sept. 1997. The **ΔcciN.n** response played remained close to the **Base.n** response. The **Δtcm1yN.n** and **ΔcciN.n** risk factor responses largely offset each other. The investors' reluctance to fully incorporate earnings growth into the price **ΔEGN.n** and investors' response to the FED tightening **Δtcm1yN.n**, reduced the **Full.n** response relative to the **Base.n** in Sept 1987 to a level close to the **sp500.n**. In the last quarter of 1987, continued FED tightening and the decline in earnings brought the **Full.n** price prediction close to the **sp500.n** at the beginning of the year, in close agreement with the **sp500.n** year-end price. There is no need to attribute the price movements in 1987 to investor irrationality if investors valued the S&P 500 using the E/P yield.

Fig. 4.3.1.E
1987: E/P

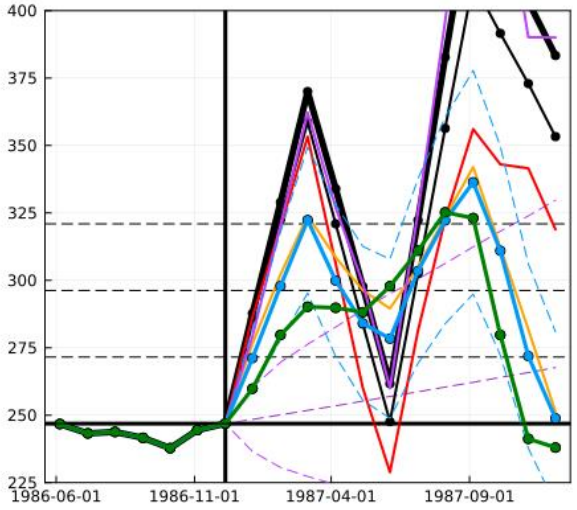
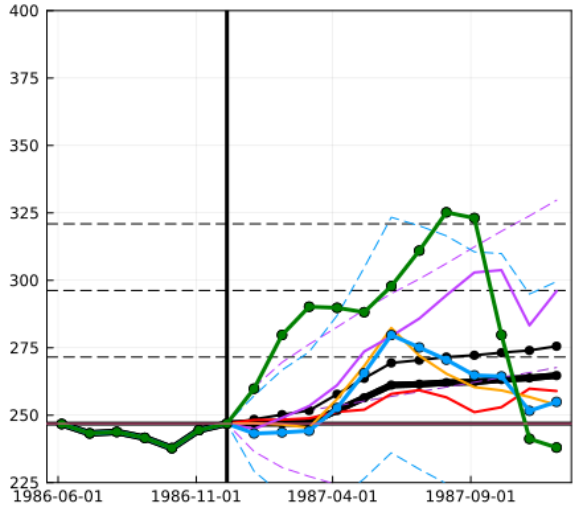


Fig. 4.3.1.D
1987: D/P



Variance Bounds: Mean.n; StdDevP.n; StdDevM.n ----; **Basic Data:** sp500.n -●-●-; **Const($X/P).n** ——

Valuation Adjust: Base.n-●-●-; Δtcm1yN.n ——; Δ$XGN.n ——; ΔcciN.n —— **Prediction:** Full.n-●-●-; StdErr.n----

Note. The good fit using E/P Is the result of the price following the earnings. Note the role of EGN in inhibiting the full impact of the earnings growth and the continuing FED tightening for the sp500 price decline in the last quarter of 1987. Consumer confidence played almost no role in the price dynamics.

4.3.2 Recessions

Recessions are periods (dated by a committee) when the real economy contracts. Textbook recessions occur when the price decline (ΔP/P) significantly exceeds the dividend decline (ΔD/D). This paper categorizes the eight recessions in the database into three basic types: textbook recessions, where the price decline decrease exceeds 1.0***StdDevM.n** boundary, quasi-textbook recessions, where the price decrease straddles the 1.0* **StdDevM.n** boundary, and non-textbook recessions, where only modest price declines occurred. The start date of the price response is the time when the price begins to decline rapidly, which is close to but not always equal to the official start date of the recession. The **vertical red line** marks the recession's official start, and the **vertical black line** marks the start date used in the price response prediction. If a black vertical line does not appear on the plot, the response prediction starts at the official start date of the

recession. To study each plot, follow the guidelines in Part 4.2 above. The textbox below the figure briefly discusses the quality of the fit and features specific to that recession. A general summary of the findings follows the plots.

Fig. 4.3.2.E

1970: E/P

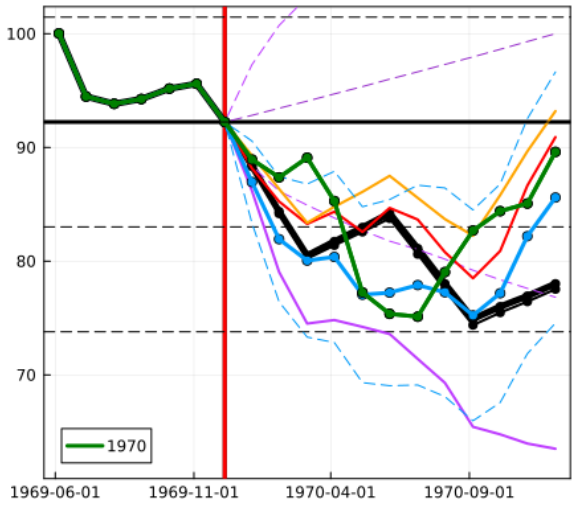
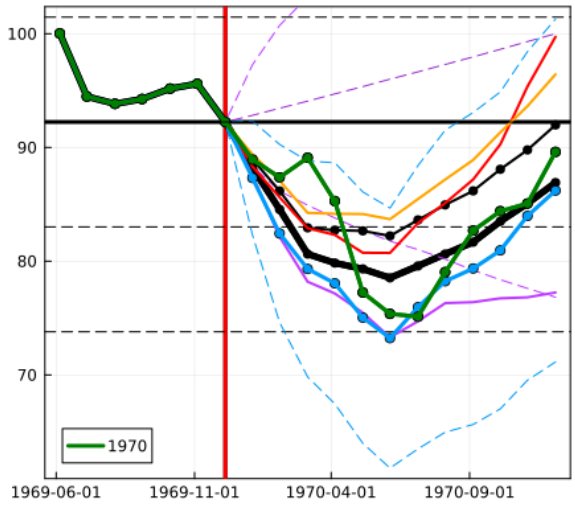


Fig. 4.3.2.D

1970: D/P



Variance Bounds: Mean.n; StdDevP.n; StdDevM.n ----; **Basic Data:** sp500.n -•-•-; **Const($X/P).n** ——

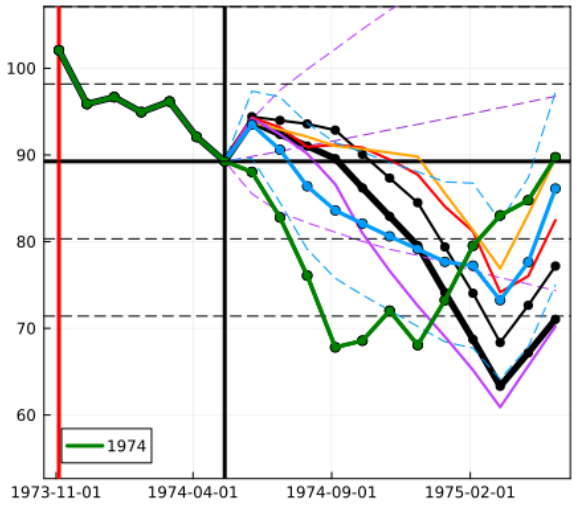
Valuation Adjust: Base.n-•-•-; ΔtcmlyN.n ——; Δ$XGN.n ——; ΔcciN.n —— Prediction: Full.n-•-•-; StdErr.n----

Note. **The 1970 Regression** was notable because there was a significant decline in the dividend comparable to the earnings decline. Both the E/P and the D/P Models closely fitted the price data. The dividend decline was likely a seasonal effect.

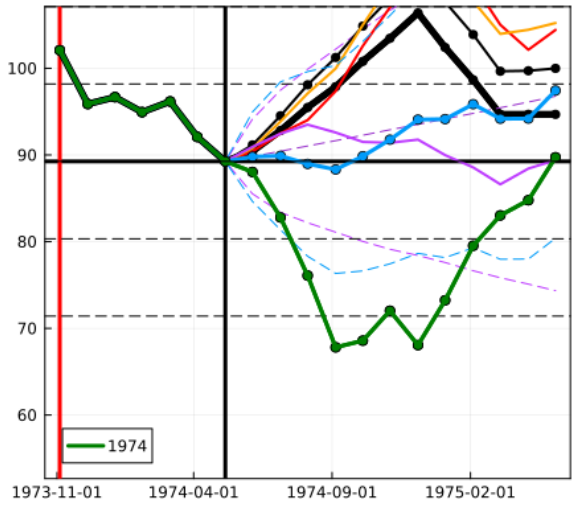
Fig. 4.3.2.D

Fig. 4.3.2.E

1974: E/P



1974: D/P



Variance Bounds: Mean.n; StdDevP.n; StdDevM.n ----; **Basic Data:** sp500.n -•-•-; **Const($X/P).n** ——

Valuation Adjust: Base.n-•-•-; ΔtcmlyN.n ——; Δ$XGN.n ——; ΔcciN.n —— Prediction: Full.n-•-•-; StdErr.n----

Note. **The 1974 Regression** was a textbook regression. The dividends increased while the price decline exceeded the 1.0 StdErr boundary. The dividend increase was possibly a seasonal effect. The Full E/P prediction declined more slowly than the price response and bottomed one quarter later.

Fig. 4.3.2.E
1980: E/P

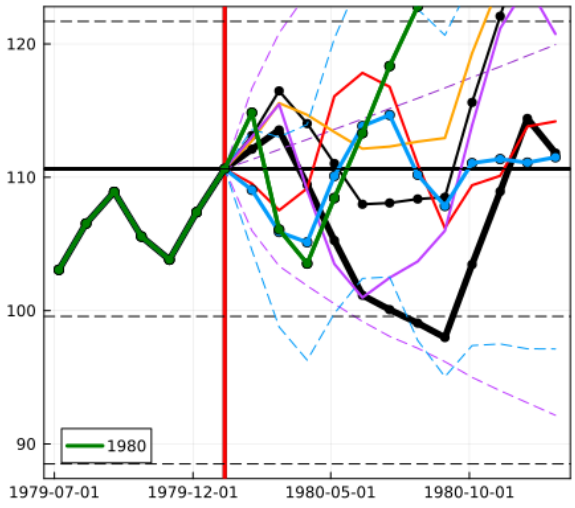
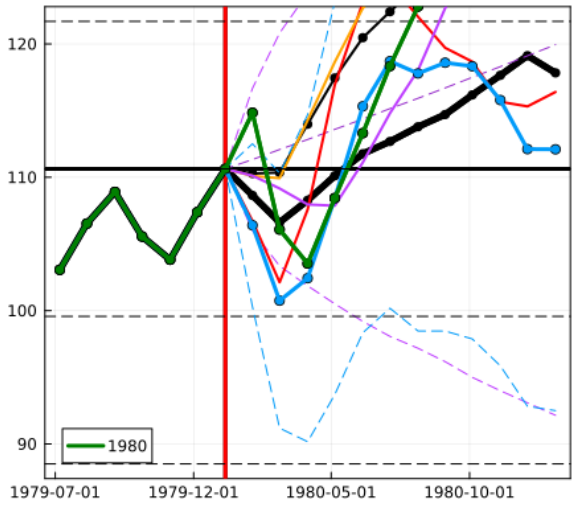


Fig. 4.3.2.D
1980: D/P



Variance Bounds: Mean.n; StdDevP.n; StdDevM.n ----; **Basic Data:** sp500.n -●-●-; **Const($X/P).n** ——

Valuation Adjust: Base.n-●-●-; Δtcm1yN.n ——; Δ$XGN.n ——; ΔcciN.n —— **Prediction:** Full.n-●-●-; StdErr.n----

Note. **The 1980 Regression** ended in May 1980 and was hardly a price regression. Both Models followed the price dip (-5%) well. Neither Model followed the rapid price increase after the recession's end.

Fig. 4.3.2.E
1981: E/P

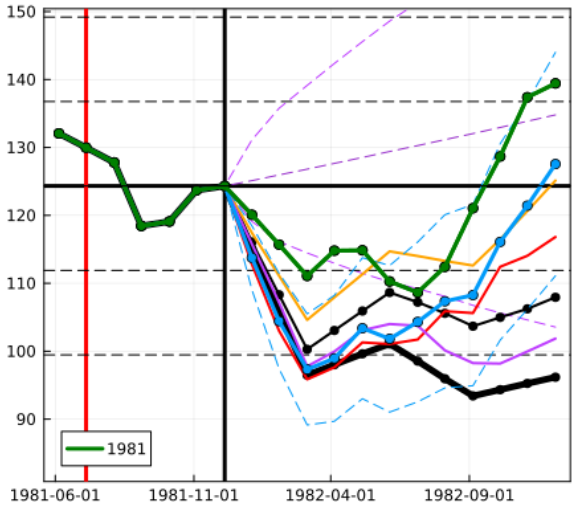
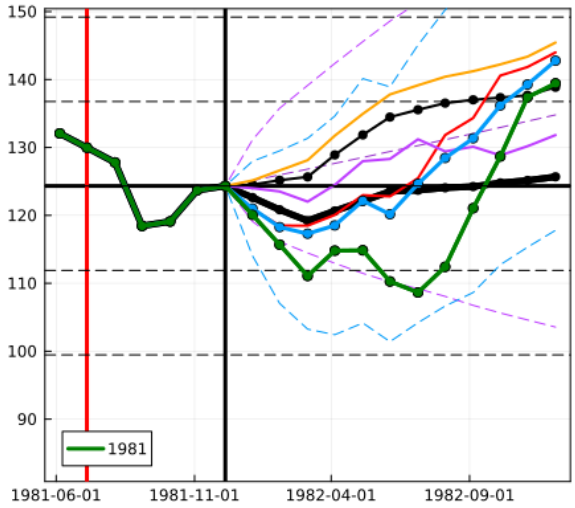


Fig. 4.3.2.D
1981: D/P



Variance Bounds: Mean.n; StdDevP.n; StdDevM.n ----; **Basic Data:** sp500.n -●-●-; **Const($X/P).n** ——

Valuation Adjust: Base.n-●-●-; Δtcm1yN.n ——; Δ$XGN.n ——; ΔcciN.n —— **Prediction:** Full.n-●-●-; StdErr.n----

Note. **The 1981 Regression** was a quasi-textbook recession because the price fell only about 10% during the first seven months. The E/P model predicted a more significant decline than the realized price decline.

Fig. 4.3.2.E
1990: E/P

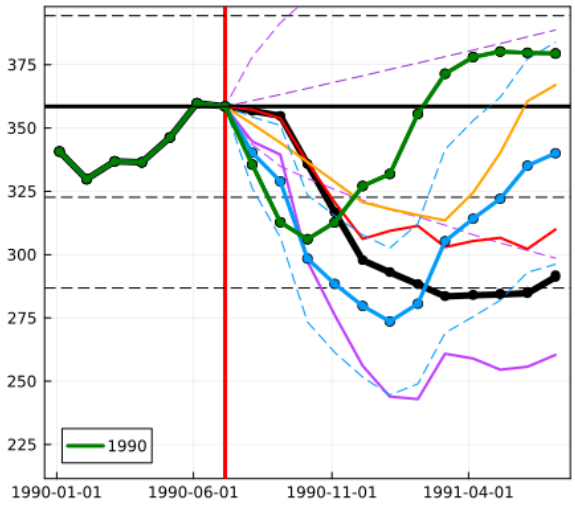
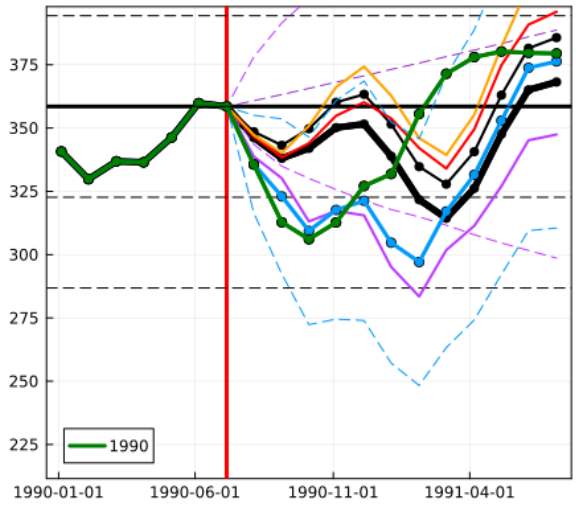


Fig. 4.3.2.D
1990: D/P



Variance Bounds: Mean.n; StdDevP.n; StdDevM.n ----; **Basic Data:** sp500.n -•-•-; **Const($X/P).n** ——

Valuation Adjust: Base.n-•-•-; ΔtcmlyN.n ——; Δ$XGN.n ——; ΔcciN.n —— Prediction: Full.n-•-•-; StdErr.n----
Note. **The 1990 Regression** price decline was rapid and shallow (-15%) and reversed about three months into the recession. The E/P Model overstated the decline and was late on the reversal. The D/P Model was significantly closer to the price trajectory.

Fig. 4.3.2.E
2001: E/P

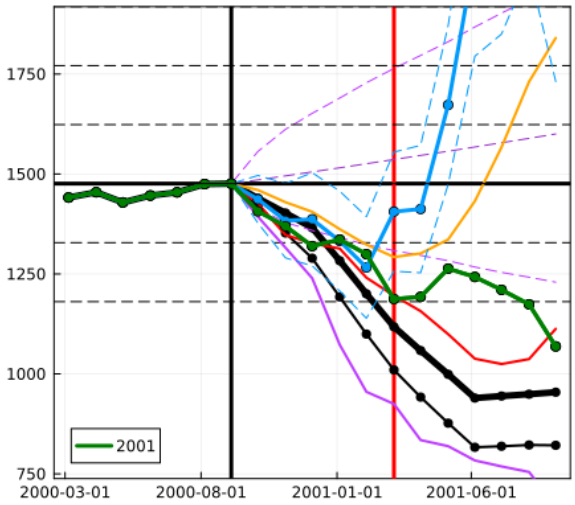
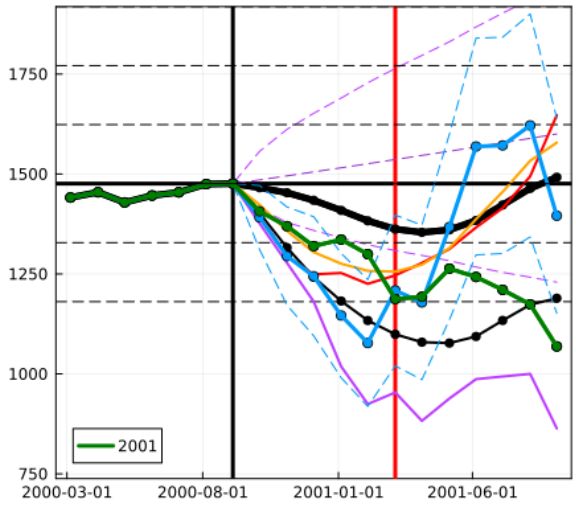


Fig. 4.3.2.D
2001: D/P



Variance Bounds: Mean.n; StdDevP.n; StdDevM.n ----; **Basic Data:** sp500.n -•-•-; **Const($X/P).n** ——

Valuation Adjust: Base.n-•-•-; ΔtcmlyN.n ——; Δ$XGN.n ——; ΔcciN.n —— Prediction: Full.n-•-•-; StdErr.n----
Note. **The 2001 Recession** price decline started significantly before the official start of the regression. The E/P Model prematurely reversed due to the FED easing and the EGN's resistance to rapid change. The D/P Model declines more slowly and reverses more gradually than E/P.

Fig. 4.3.2.E
2008: E/P

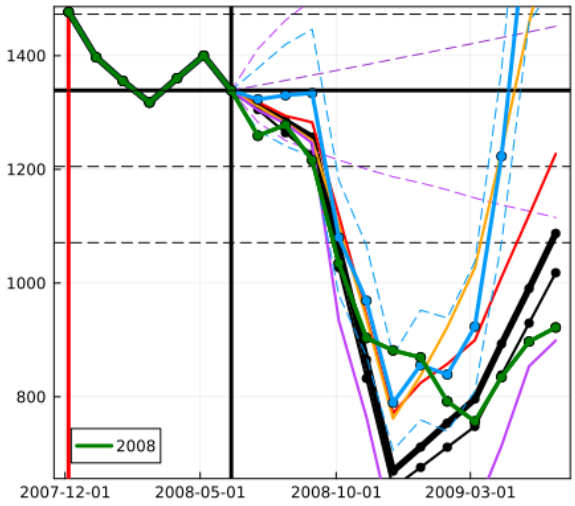
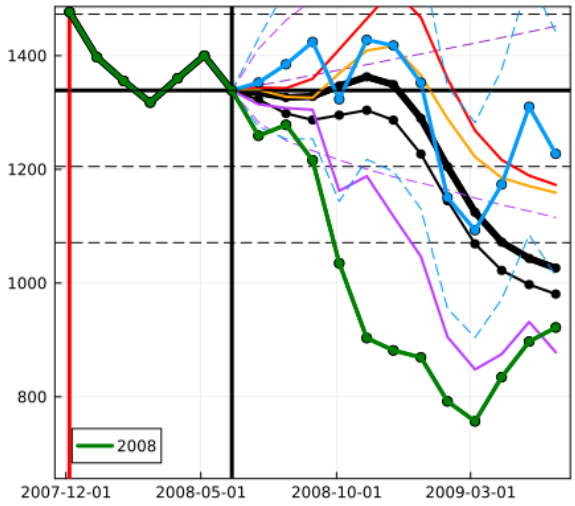


Fig. 4.3.2.D
2008: D/P



Variance Bounds: Mean.n; StdDevP.n; StdDevM.n ----; **Basic Data:** sp500.n -●-●-; **Const($X/P).n** ——

Valuation Adjust: Base.n-●-●-; Δtcm1yN.n ——; Δ$XGN.n ——; ΔcciN.n —— **Prediction:** Full.n-●-●-; StdErr.n----

Note. **The 2008 Recession's** rapid price decline started more than six months after the recession's official start, declining more than 40% after the Lehman bankruptcy. The earnings for the last quarter of 2008 were adjusted to prevent a negative price forecast (see Appendix A.2). The E/P model using the adjusted earnings followed the decline and recovery very well. The D/P Model trajectory predicted only a modest price decline.

Fig. 4.3.2.E
2020: E/P

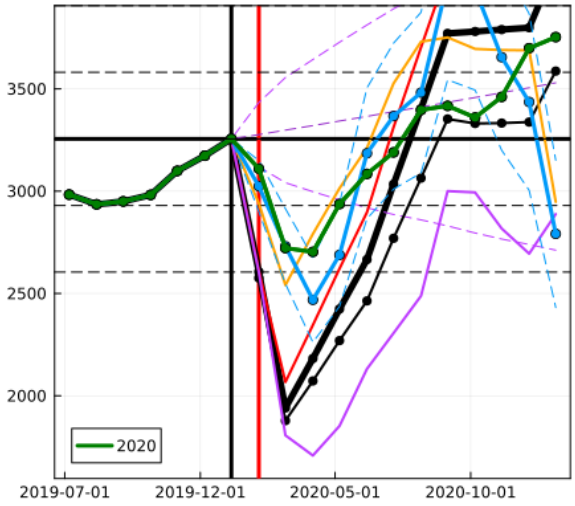
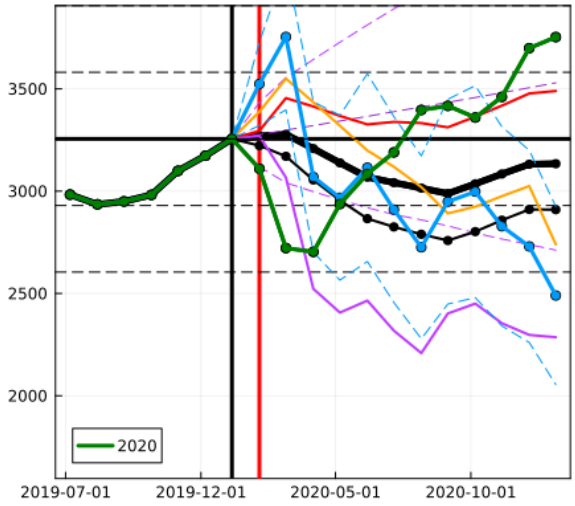


Fig. 4.3.2.D
2020: D/P



Variance Bounds: Mean.n; StdDevP.n; StdDevM.n ----; **Basic Data:** sp500.n -●-●-; **Const($X/P).n** ——

Valuation Adjust: Base.n-●-●-; Δtcm1yN.n ——; Δ$XGN.n ——; ΔcciN.n —— **Prediction:** Full.n-●-●-; StdErr.n----

Note. **The 2020 Recession** price decline occurred within a single quarter, followed by almost a complete recovery one quarter later. The E/P Model prediction closely follows the price trajectory. The D/P Model trajectory continued to decline throughout the 12-month forecast horizon.

Analysis of Recessions

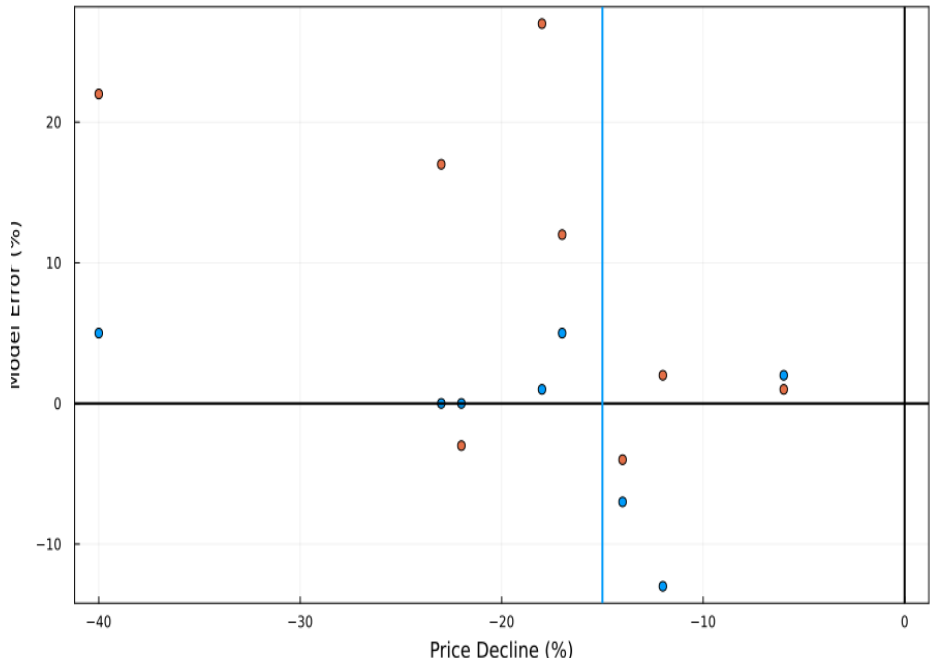
Recession Types: In the textbook recessions (1974, 2008, and 2020), the quality of the E/P fit (**Full.E.n**) to the price history (**sp500**) greatly exceeds the quality of the D/P fit (**Full.D.n**). In quasi-textbook recessions (1981, 1990, and 2001), the quality of the E/P fit is better than the D/P fit, but a definitive statistical decision is impossible. In non-textbook recessions (1970, 1980), where the payout ratio did not change significantly, the quality of the price response fits for E/P and D/P are similar."

Risk Factors: As the FED aggressively lowers interest rates and consumer confidence declines, the price responses due to the **Δtcm1yN.n** and **Δtcm1yN.n** risks have opposite signs and largely offset each other. The price changes due to the **Δ$XGN.n** risks differ. Because the volatility of the dividend stream is low, the price change due to the **ΔDGN.n** risk is negligible. In contrast, the resistance to incorporating the earnings decline in the **ΔEGN.n** risk is crucial in providing a good fit in the textbook recessions.

Figure 4.3.3 plots (estimates of) the maximum price decline against the E/P and D/P response error at the point of the maximum decline. The vertical line indicates the value of StdDev(ΔP/P.12) at a twelve-month horizon. In regressions where the price decline (ΔP/P.12) exceeds StdDev(ΔP/P.12), the E/P Model has low errors compared to the significant positive errors of the D/P Model. The confidence factor (**ΔcciN.n**) in the D/P Model is not large enough to explain the price decline.

Fig. 4.3.2

Analysis of Recessions



E/P Model Error ● ; D/P Model Error ●

Note. Analysis of the recession fit error. Vertical blue line is **StdDev(ΔP/P.12)**

4.3.3 Internet Era: Was there a 'Bubble'?

In the last years of the 1990s, equity prices appeared to increase irrationally. People colloquially attributed the rapidly increasing prices to the onset of an 'Internet Era,' during which equity prices could continue to increase ad infinitum. The plots below analyze the price increases during the years that marked the beginning (CY1997) and the end (CY1999) of the 'Internet Era.'

Fig.4.3.3.1 analyzes the first year of the Internet Era. The **sp500.n** rose about 30% during the year, while the **Const($X/P.n)** line shows that earnings and dividends were almost flat. The **Base.n** lines were close to the **Const($X/P.n)** lines because $X/P ~<$X/P>. The **Δtcm1yN.n** lines show that the FED did not significantly change the short risk rate. The **ΔcciN.n** lines show that the

rapid increase in consumer confidence drove the rapidly increasing price throughout the year. The Model prediction, however, was well within the Model StdErr.

Fig. 4.3.3.1.E

Internet Era 1997: E/P

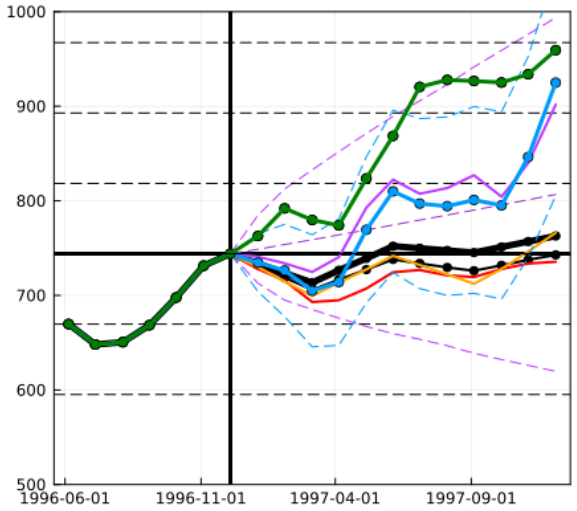
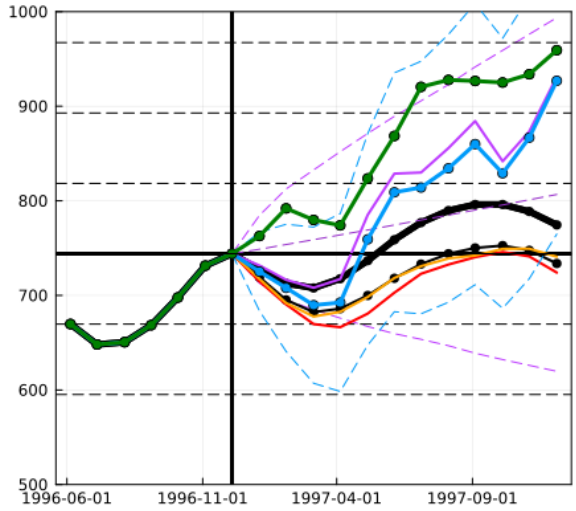


Fig. 4.3.3.1.D

Internet 1997: D/P



Variance Bounds: Mean; StdDevP; StdDevM ——; **Basic Data:** sp500-●-●-; **Const($X/P)**----
Valuation Adjustments: Base-●-●-; Δtcm1yN.n----; Δ$XGN.n----; ΔcciN.n---- Prediction: Full-●-●-; StdErr ——
Note. See main text.

Fig. 4.3.3.2 shows CY 1999, the final year of the Era. The **sp500.n** increased another 20% by the end of the year. The **Const(E/P.n)** line shows that earnings also increased by 20% throughout the year. However, in contrast to 1997, there was a large gap between the **Base.n** and the **Const(E/P.n)** lines due to the extreme values of E/P.0 >> Mean(E/P); this places a significant return-to-the-mean nudge into the prediction. Despite the large increase in consumer confidence **ΔcciN.n**, the model prediction (**Full line**) was flat for the year due to the negative effect of rising short-term interest rates **Δtcm1yN.n,** and the resistance to incorporating the earnings growth **Δ$XGN.n**.

The classic definition of a 'bubble' is the failure of investors to recognize the return to the mean. Such a failure occurred during the late stages of the Internet bubble.

Fig. 4.5.2.D
Internet 1999: E/P

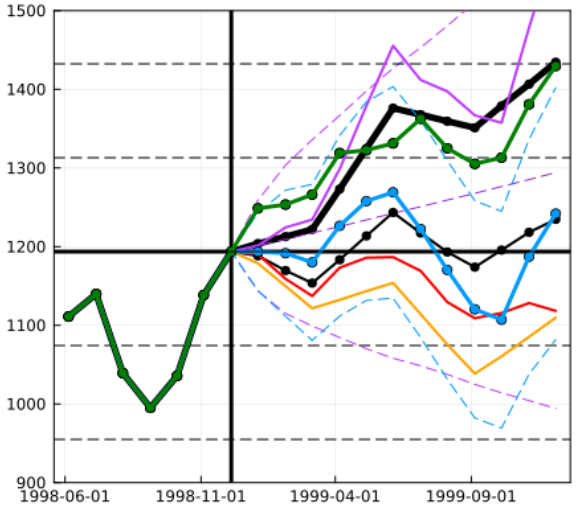
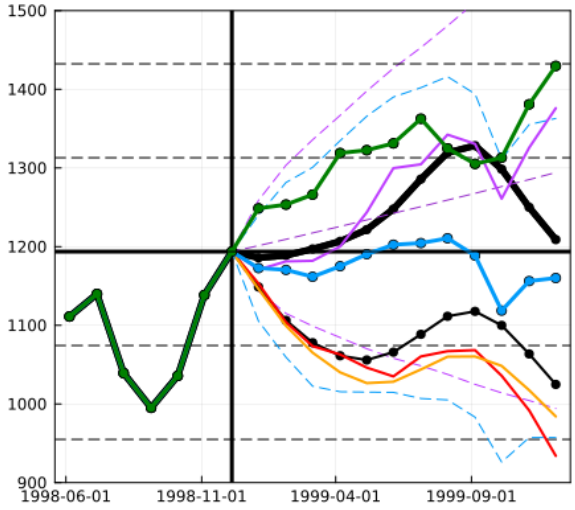


Fig. 4.5.2.D
Internet 1999: D/P



Variance Bounds: Mean; StdDevP; StdDevM ——; **Basic Data:** sp500-●-●-; ----
Valuation Adjustments: Base-●-●-; Δtcm1yN.n----; Δ$XGN.n----; ΔcciN.n---- **Prediction:** Full-●-●-; StdErr ——
Note. See main text

5. Why do the 3MR Risk Variables have Such Large Explanatory Value?

In the static regression Y_{3MR} (Eq. 4), the yield covaries directly with the 3MRi risk variables, and the entire volatility risk of the dataset affects the investor. The Y_{3MR} regression does not explain the sizeable explanatory value of the 3MRi risk variables. Discount models, on the other hand, have time-varying parameters that provide an economic explanation for the yield variance. Functionally connecting the parameters of a microfounded discount model to the 3MRi risk variables connects the two Models.

5.1. Calibrating the Parameters of a MicroFounded Model

Consider the following specification for a micro-founded discount model Y_{MF}, which resembles the Model studied by Campbell and Shiller (1989) in their paper describing the LogLinear Model.

$$Y_{MF}: \frac{\$X}{P} = (r_{rf} + \gamma\mu) - \mu \qquad (6)$$

The SDF (the term in parentheses) contains three risk parameters: γ is the relative risk aversion, r_{rf} is the risk-free rate, and μ is the growth expectation. Campbell and Shiller used the real risk-free rate. Motivated by the sizeable explanatory value of tcm1yN in the 3MR Model, here, r_{rf} is the nominal risk-free rate tcm1y. The microeconomic literature refers to the product γμ as the Resistance to Intertemporal (RtoIS). The RtoIS value marks the boundary where consumers are indifferent between selling (consuming now) or waiting another period, expecting to receive greater consumption due to consumption growth.

The Y_{MF}'s parameters become time-varying when functionally connected to the time-varying risk variables. The 'natural' functional associations are γ = γ(cciN), μ = μ($XGN), and r_{rf} = r_{rf}(tcm1yN). First-order expansions expose $X/P directly to the risks, e.g., $\gamma = \gamma_0 + \frac{\partial \gamma}{\partial (cciN)} \boldsymbol{cciN_t}$. Substituting into Eq. 6 results in a first-order equation for Y_{MF} linear in the 3MRi

$$Y_{MF}: \frac{\$X}{P} = \text{Constant} + StdDev(tcm1y) * tcm1yN + (\gamma_0 - 1)\frac{\partial \mu}{\partial (\$XGN)}\$XGN + \mu_0 \frac{\partial \gamma}{\partial (cciN)} cciN \qquad (7)$$

where the $Constant = ([(< tcm1y > + (< \gamma > -1) < \mu >]$. Requiring Y_{MF}=Y_{3MR} calibrates the functional connections. Table 5.2.1 illustrates the calibration of the gradients.

Table 5.2.1 Calibration of the Gradients: Eq. 8a, 8b and 8c

$$\frac{\partial r_{nom}}{\partial (tcm1yN)} = ß_{(3MR,tcm1yN.)} \qquad \frac{\partial \gamma}{\partial (cciN)} = \frac{ß_{(3MR,cciN)}}{\mu_0} \qquad \frac{\partial \mu}{\partial (\$XGN)} = \frac{-ß_{(3MR,\$XGN)}}{(\gamma_0 - 1)}$$

Table 5.2.2 shows the calibrated functional connections.

Table 5.2.2 Functional Connections: Eq. 9a, 9b and 9c

$$r_{nom} = < tcm1y > + ß_{(tcm1yN)} * \text{tcm1yN} \quad \gamma = < \gamma > + \frac{ß_{(cciN)} * cciN}{\mu_0} \quad \mu = \mu_0 + \frac{-ß_{(\$XGN)} * \$XGN}{(\gamma_0 - 1)}$$

Noting that <$X/P> and <tcm1y> are known from the data and assuming <μ> = <$XG>, zero-order equality requires $< \gamma >= 1 + \frac{<\frac{\$X}{P}> - <tcm1y>}{<\$XG>}$. Using the empirical values [<EG>=6.44%,

<DG>=5.50%, <tcm1y> = 4.99%, <E/P>=6.86%, and <D/P>=2.90%], zero-order estimates the mean risk aversions as $< \gamma_E > = 1.29$ and $< \gamma_D > = 0.63$.

For Y_{3MR} to be interpretable as a discount equation, the $ß_{\$XGN}$ calibration requires the minus sign. Using the estimates for <γ> and the $\beta_{3MR}(s)$ in Table 2.1.1, both StdDev(γ)/<γ> < 1 and StdDev(μ)/<μ> < 1, so both vary within moderate ranges around their means. A large value of <γ> is not necessary to explain the volatility of $X/P when the risk variables are volatile. The γμ represents the excess expected return if and only if the investor expects to hold the equity in perpetuity and expects the state of risk will not change.

5.2. Connecting the Reactive and the Static Models

Subtraction calculates the intertemporal change in the Y_{MF} parameters (Table 5.2.2): $\Delta\gamma = \frac{ß_{(cciN)} * \Delta cciN}{\mu_0}$ and $\Delta\mu = \frac{-ß_{(\$XGN)} * \Delta \$XGN}{(\gamma_0 - 1)}$. Subtraction works because, in the static limit, $ß_{cciN}$ and $ß_{\$XGN}$ do not depend on the horizon. Using the calibrations in Table 5.2.2, Δ$X/P.n is

$$\Delta \frac{\$X}{P}.n = \Sigma_i ß_{3MRi} * \Delta 3MRi.n \tag{10}$$

The $ß_{3MRi}$ are large (see Table 2.1) because the static reactive change exposes the investor to the entire yield variance of the dataset.

In the Taylor limit, the exposure to variance risk increases with the horizon, and the predicted change in the yield increases with the horizon.

$$\Delta \frac{\$X}{P}.n = \Sigma_i ß_{\Delta 3MRi.Taylor.n} * \Delta 3MRi.n \tag{11}$$

The $ß_{\Delta 3MRi.n}$ increase with the horizon, but the increases begin to saturate as $ß_{\Delta 3MRi.n}$ approaches $ß_{3MRi}$ (see Fig. 2.4.1).

The investor's horizon explains why the 3MRi risk variables are potent predictors of changes in Δ($X/P). If the investor has a short horizon, the price change return forms the basis of the expected return, so the investors choose to ignore the return from the dividend; investors react to each 3MRi risk upon its report. Investors with a long-horizon view, for whom the dividend return is essential, calculate the long-horizon expected return by discounting the expected dividend stream. The time variation of the SDF in the discount model arises because the 3MRi risks influence its parameters, resulting in high time-varying expected returns and, consequently, a high volatility for the valuation.

6. Summary

The 3MR Reactive Price Model (Model) connects changes in the monthly risk-adjusted S&P 500 index (P) to changes in **3 M**acro **R**isk data variables: the one-year treasury bond rate (*tcm1yN*), the consumer confidence index (*cciN*) and the trailing earnings growth rate *($XGN*) [derived from the monthly S&P 500 index earnings]. The values of the 3MRi triplet define 'the state of risk' of the macrofinance economy. The price change is a two-step process. In the first step, targeted investors who receive the news that one of the 3MR data variables has changed reactively re-estimate the earnings yield $X/$P_{Estimate.t}$. In the second step, the investor applies the estimate to $\$X_t$ to change the price ($P_t=\$X_t/(\$X/P_{Estimate.t})$). Reactive regressions calculate the strength of the responses $ß_{\Delta 3MRi.n}$ arising from the Δ3MRi changes. If the investor who receives the news is in the future, investors in the current time step can predict the price using their expectations for $\$X_{t+n}$ [=>XGN_{t+n}$], tcm1yN$_{t+n}$, and cciN$_{t+n}$. When the Model includes memory, there are three horizon regimes: small (Taylor): the model uses only previous values of X/P_t$, intermediate: the model uses both X/P_{t-n}$ and <$X/P> and *long:* the model uses only <$X/P>. The

response strengths ($ß_{\Delta 3MRi.n}$) and the ΔYIPE.n errors increase with the horizon, and both saturate as they approach their static limits. The Model predicts a price density centered on the regression prediction with a standard error comparable to the price change volatility. When E/P is the valuation ratio, the Model price predictions follow the large price changes during 1987 and the recessions in the database. The memory effect in the Full model explains the high prices that occurred during the 'Internet Era. A study of the 3MR variables as the natural drivers of change in the three foundational parameters of a microfounded consumption model explains their significant explanatory power.

Predictability required abandoning the two equity pricing paradigms that dominate in the current literature.

1. The equity pricing process is purely forward-looking. In the 3MR Reactive Price Model, the pricing process is backward-looking.
2. Equity price changes follow a Martingale process, so equity price change expectations vary randomly. In the 3MR Reactive Price Model, price changes result from changes in the macrofinance 'state of risk' and are predictable.

The 3MR Reactive Price Model fills the large gap in the literature between the sub-monthly horizon, where the martingale property may be appropriate, and the long horizon literature, where investors have lost memory of previous valuations and risk variables. In the gap filled (horizons 1:12 months), expectations for changes in the price of the market portfolio (S&P 500) are a primary subject of discussion in the financial press.

The usefulness of the 3MR Reactive Price Model to investors making portfolio adjustments depends on both the Model prediction error and the investor's ability to forecast future values for the 3MRi.n risk variables and the reference cash data variable ($X.n). Prediction errors at horizon n are comparable to the price change volatility (StdDev(ΔP/P.n)) at that horizon; the size of the

error limits but does not preclude application. I expect error reduction will become the next research frontier.

References

Adam, Klaus, and Stefan Nagel, (2023). Expectations Data in Asset Pricing. Handbook of Economic Expectations, 477-506.

Black, Fischer, and Myron Scholes, 1973. The Pricing of Options and Corporate Liabilities. Journal of Political Economy 81: 637-654.

Bordalo, Pedro, Nicola Gennaioli, and Andrei Shleifer, 2022. Overreaction and Diagnostic Expectations in Macroeconomics. Journal of Economic Perspectives 36: 223-244.

Bordalo, Pedro, Nicola Gennaioli, Rafael La Porta, and Andrei Shleifer, 2024. Belief Overreaction and Stock Market Puzzles. Journal of Political Economy 132: 5.

Bordalo, Pedro, Nicola Gennaioli, Rafael La Porta, Matthew O'Brien, and Andrei Shleifer, 2023. Long Term Expectations and Aggregate Fluctuations. NBER Working Paper No. 31578.

Campbell, John Y., and Robert J. Shiller, 1988. The Dividend-Price Ratio and Expectations of Future Dividends and Discount Factors. The Review of Financial Studies 1: 195-228.

Chinco, Alex, Samuel M. Hartzmark, and Abigail B. Sussman, 2022. A New Test of Risk Factor Relevance. The Journal of Finance 77: 4.

De La O, R., and S. Myers, 2021. Subjective Cash Flows and Discount Rates. Journal of Finance 76: 1339-1387.

De La O, Ricardo, and Sean Myers, 2023. Which Subjective Expectations Explain Asset Prices? USC Marshall School of Business Research Paper Sponsored by iORB, No. Forthcoming. Available at SSRN: https://ssrn.com/abstract=3867773 or http://dx.doi.org/10.2139/ssrn.3867773.

Dew-Becker, Ian, and Stefano Giglio, 2024. Recent Developments in Financial Risk and the Real Economy. Annual Review of Financial Economics 16. https://doi.org/10.1146/annurev-financial-082123-105456.

Malkiel, Burton G., 2003. The Efficient Market Hypothesis and Its Critics. Journal of Economic Perspectives 17: 59-82.

Nagel, Stefan, and Zhengyang Xu, 2022. Asset Pricing with Fading Memory. The Review of Financial Studies 35: 219-245.

Samuelson, Paul A., 1965. Proof That Properly Anticipated Prices Fluctuate Randomly. Industrial Management Review 6: 41.

Appendix A Data Sources and Definitions

A.1 Definitions

The S&P 500 risk-adjusted monthly price is $P \equiv (P_{begin} + P_{high} + P_{low} + P_{end})/4$

The Model identifies normalized data variables using a trailing 'N' and defines them as $xiN \equiv (xi - \langle xi \rangle)/StdDev(xi)$.

The paper organizes its content into Parts (1,2,..) and Subparts (1.1, 1.2,..). The document keys Tables and Figures to the Subparts in their numerical order, e.g., Fig. 4.2.1, Fig. 4.2.2.

The year-over-year trailing growth rate $XG ≡ ($X(t)-$X(t-12))/$X(t-6).

A.2 Data Sources

Yahoo Finance provided the historical monthly S&P 500 price data[2].

The S&P 500 spreadsheet[3] provided quarterly S&P 500 earnings data starting from the first quarter of 1988. A list of quarterly S&P 500 earnings before 1988 is available only from Standard and Poor Inc. via subscription. This paper uses a workaround suggested by a blogger to *estimate* the quarterly earnings before 1988.[4] The method extrapolates backward from 1988 using the Shiller spreadsheet.[5] Comparisons of the estimates with the Standard and Poor quarterly earnings data displayed in a time-series chart published by Yardeni Research[6] support the accuracy of the extrapolation method. Because the earnings for the last quarter of 2008 were negative, the last quarter of 2008 earnings have been replaced with a value that results in an S&P Price consistent with the book value of the S&P 500. The replacement results in the rounded bottom for the predicted price in Fig. 4.3.2.E. This adjustment is the only data adjustment made in this paper. Linear extrapolation yielded the monthly earnings, assuming the company reports quarterly earnings in the last month of the quarter.

---

[2] https://finance.yahoo.com/

[3] https://www.spglobal.com > additional material

[4] https://politicalcalculations.blogspot.com/2013/02/quarterly-data-for-s-500-since-1871.html.

[5] http://www.econ.yale.edu/~shiller/data.htm

[6] https://yardeni.com/charts/sp-500-growth-paths/

The FRED interest rate tables provide the tcm1y data. A commercial source provided the Consumer Confidence Index (CCI) data. The historical database restricts the start date to 1967:1-2022:12 to align with the start of the CCI data series.